



VCU

Virginia Commonwealth University
VCU Scholars Compass

Theses and Dissertations


Graduate School

2017

An Investigation of Surface Characteristics of Enamel Treated with Infiltrative Resin: A Scanning Electron Microscopy Study

Danielle E. Easterly
Virginia Commonwealth University

Follow this and additional works at: <https://scholarscompass.vcu.edu/etd>

 Part of the [Dental Materials Commons](#), [Oral Biology and Oral Pathology Commons](#), [Orthodontics and Orthodontology Commons](#), and the [Other Dentistry Commons](#)

© Danielle E Easterly

Downloaded from

<https://scholarscompass.vcu.edu/etd/4764>

This Thesis is brought to you for free and open access by the Graduate School at VCU Scholars Compass. It has been accepted for inclusion in Theses and Dissertations by an authorized administrator of VCU Scholars Compass. For more information, please contact libcompass@vcu.edu.

© Danielle Easterly 2017

All Rights Reserved

An Investigation of Surface Characteristics of Enamel Treated with Infiltrative Resin:
A Scanning Electron Microscopy Study

A thesis submitted in partial fulfillment of the requirements for the degree of Master of Science
in Dentistry at Virginia Commonwealth University.

By

Danielle E. Easterly
B.A., Psychology, University of Virginia, 2010
D.D.S., Virginia Commonwealth University, 2015

Director: Dr. Eser Tüfekçi,
D.D.S., M.S., Ph.D., M.S.H.A.
Professor, VCU Department of Orthodontics

Virginia Commonwealth University
Richmond, Virginia
May 2017

Acknowledgement

The author wishes to express gratitude to many people. First and foremost, thank you to my mother and father, Margo and Jim Easterly, and to my fiancé Andrew Robb, for their constant support and encouragement. I would also like to extend a large thank you to Jennifer Shim for all her help in preparing the samples and for her help in data preparation. Thank you to Dr. Dmitry Pestov for all of his guidance and expertise in the area of nanomicroscopy and materials. Thank you to Judy Williamson for completing the SEM analysis of all the samples in the study. Thank you also to Dr. Robert Seghi of The Ohio State University for his guidance and donation of the toothbrush simulator. Last but very importantly, thank you to my thesis advisor Dr. Eser Tüfekçi for her motivation, guidance, and friendship.

Table of Contents

Acknowledgement	ii
Table of Contents	iii
List of Figures	iv
List of Tables	v
Abstract	vi
Introduction.....	1
Materials and Methods.....	6
Results.....	11
Discussion	21
Conclusions.....	30
Literature Cited	31
Appendix: SEM Images of Extracted Teeth	36
Vita.....	61

List of Figures

Figure 1: Confirmation of WSLs on Pilot Teeth	7
Figure 2: Mounting of tooth under toothbrush simulator.	8
Figure 3: Baseline Image of Sound Enamel. Tooth B. 250X Magnification.....	11
Figure 4: Baseline Image of Demineralized Enamel. Tooth C. 250X Magnification.	12
Figure 5: Tooth 2. Location B. T1. 250X Magnification.....	13
Figure 6: Tooth 4. Location B. T1. 250X Magnification.....	13
Figure 7: Tooth 10. Location B. T1. 250X Magnification.....	13
Figure 8: Changes in Presence of Enamel Rods After Simulated Brushing.....	15
Figure 9: Changes in Presence of Microcracks After Simulated Brushing	16
Figure 10: Changes in Presence of Fractures After Simulated Brushing	18
Figure 11: Association between Enamel Rods and Microcracks.....	19
Figure 12: Association between Enamel Rods and Fractures.....	20
Figure 13: Tooth 2. Location B. T1 (left) and T2 (right). 250X Magnification.	22
Figure 14: Comparison between T1 (left) and T2 (right) of Tooth 4. Location C. 250X Magnification.....	23
Figure 15: Tooth 1. Location B. T1. 250X Magnification.....	25
Figure 16: Tooth 3. Location B. T2. 250X Magnification.....	25
Figure 17: Tooth 6. Location B. T1. 250X Magnification.....	25

List of Tables

Table 1: Distribution of SEM Characterizations between T1 and T2	14
--	----

Abstract

AN INVESTIGATION OF SURFACE CHARACTERISTICS OF ENAMEL TREATED WITH INFILTRATIVE RESIN: A SCANNING ELECTRON MICROSCOPY STUDY

Danielle E. Easterly, Doctorate of Dental Surgery.

A thesis submitted in partial fulfillment of the requirements for the degree of Master of Science in Dentistry at Virginia Commonwealth University.

Virginia Commonwealth University. 2017.

Director: Dr. Eser Tüfekçi
D.D.S., M.S., Ph.D., M.S.H.A.

Objective: To evaluate the microstructural changes of a resin infiltrant (ICON®, DMG America LLC, Englewood, NJ) after six months of simulated toothbrushing.

Materials and Methods: Ten extracted third molars (n=10) were collected. Artificial white spot lesions were created and resin applied. Environmental SEM images at 250X and 500X were taken after application of Icon® (T1), and after six months of simulated toothbrushing (T2). Micrographs were evaluated for changes in surface characteristics.

Results: SEM showed some changes in the surface characteristics of the resin after simulated toothbrushing. However, changes in presence of enamel rods, microcracks, or fractures were not

statistically significant ($p > 0.05$). The effects of polymerization shrinkage were noted on most samples in the form of clefts and fissures.

Conclusions: Icon® resin seems to withstand challenge by toothbrush abrasion over a six-month period, with some evidence of microstructural wear.

Introduction

White spot lesions (WSLs) are one of the most common unesthetic sequelae from fixed appliances, and leave clinicians with a challenge regarding their management. WSLs develop from dissolution of calcium, phosphate and fluoride ions from the enamel due to prolonged plaque retention, which results in microporosities in the remaining tooth structure.¹

Demineralized enamel takes on a white chalky appearance that represents the initial phase of caries formation prior to more extensive enamel breakdown. Previous studies reported a wide variance in prevalence of WSLs, ranging from 0 to 97%, which was thought to result from the differences in the study designs.²⁻⁴ However, a well-designed study from 2013 found that approximately 25% of patients undergoing orthodontic therapy develop a WSL during treatment.² In a recent systematic literature review, the incidence and prevalence of WSLs were reported as 45% and 68%, respectively, in orthodontic patients.⁵ Therefore, despite the development of new preventive materials and products, demineralization appears to negatively affect a significant portion of orthodontic patients.

Although it is generally accepted that patients are responsible for the prevention of WSLs, orthodontists and general dentists should educate patients at risk, and implement the appropriate preventive measures.⁶ Minimally invasive dentistry and fluoride delivery systems in the form of mouthwashes and toothpastes should be considered as the first line of defense to prevent incipient caries. In non-compliant patients, fluoride varnishes or other fluoride delivery systems can be used to arrest the caries process by decreasing the susceptibility of enamel to acid attack or even to promote remineralization.⁷ For active or arrested WSLs that are more advanced or

have been present for a longer duration, fluoride treatment is not recommended as only the external layer of demineralized enamel will harden. This will create an enamel surface that is hard and more lustrous than the initial WSL, however the loss of fluorescence at the deeper layer will largely remain, causing the appearance of a white opacity to remain on the tooth.⁸⁻¹⁰ Thus, for deeper or longstanding WSLs, different interventions need to be utilized to arrest the caries process and improve the aesthetic outcome.

Recently, an unfilled low-viscosity infiltrative resin (Icon®, DMG America LLC, Englewood, NJ) has been introduced as a non-invasive agent to diminish the appearance of WSLs and hence to improve esthetics.¹¹ One major benefit of this resin is the ability to improve the appearance of WSLs without removal of gross tooth structure, which was reflected by findings in a recent systematic literature review.¹² However, it was concluded that due to insufficient high quality studies, more research was needed to determine long-term efficacy of the infiltrative resin.

Icon®, abbreviated from “**I**nfiltration **concept**,” is composed primarily of monomer triethylene glycol dimethacrylate (TEGDMA), with solvent composed of ethanol and photoinitiators camphorquinone (CQ), and ethyl-4-dimethylaminobenzoate (DABE). The unfilled property of this infiltrative resin allows for low viscosity and a high penetration coefficient, which is necessary for the resin to penetrate completely into enamel with a small pore volume.¹³ After removal of the superficial hardened enamel layer with 15% hydrochloric acid (HCL), the application of resin over the lesion infiltrates the porosities present in the exposed demineralized enamel by capillary action. This process takes place over the course of several minutes.¹⁴ The enamel consequently is sealed off and filled from within, without requiring a protective surface layer of resin thickness, which is the primary mechanism by which other sealant products on the

market function.¹⁵ Additionally, since the porosities in the enamel are filled, which would normally serve as pathways for bacterial migration into deeper tooth structures, the resin also serves as a barrier to stop the future progression of incipient lesions by physically blocking further mechanical, bacterial, and acid attack.¹⁵

The TEGDMA in infiltrative resin is comprised of a shorter C-O backbone than other similar monomers such as Bis-GMA, which has a higher viscosity. While the shorter backbone imparts the low viscosity necessary for infiltration, it also causes a higher degree of polymerization shrinkage after light curing, especially with only a single application.¹⁶ The polymerization results in cleft-like structures embedded within the resin, which can lead to decreased acid resistance.¹⁶ Evidence shows that a repeated application of the resin can fill in these clefted areas, and also that a double application after a period of continued demineralization increases the enamel micro-hardness of the demineralized area significantly more than a single application.^{17,18} Studies have also shown that hardness for infiltrated lesions is lower than for typical glass-ionomer cements and composite resins, which could indicate an increased susceptibility for wear.¹⁸⁻²⁰ Since unfilled resins are typically not resistant to mechanical abrasion over time, it is possible that breakdown or wear of the infiltrant could take place. Therefore, there may be a need for repeated applications of the resin.

In the literature, numerous studies focused on the long-term color stability of infiltrative resin. These investigations reported that the demineralized enamel treated with the resin infiltrant becomes discolored over time when exposed to substances such as coffee and wine.²¹⁻²⁴ However, the discoloration is reversible, and upon rubber cup polishing the discolored resin treated enamel readily gains back its original color characteristics. Despite several studies on the color stability, there is only limited information available on the long-term mechanical stability

of the resin infiltrant when subjected to mechanical wear and daily abrasive challenges such as toothbrushing.

Yetkiner et al.²⁵ compared the stability of Icon® paired with different enamel adhesives on bovine teeth, challenging the material with cycles of acidic solution and toothbrush abrasion. To measure stability, the amount of calcium dissolution from the teeth over time into aqueous solution was measured. Despite showing initial stability, the amount of calcium leached from the resin treated teeth was found to increase over time. In contrast, untreated control teeth exhibited calcium dissolution at a more constant rate over time. This finding may be indicative of some mechanical breakdown of the resin infiltrant over time when challenged by an acidic environment and mechanical abrasion.

In contrast, a 2011 study investigating the toothbrush abrasion resistance of infiltrative resin applied onto demineralized bovine teeth, reported wear as a vertical loss in height compared to adjacent healthy enamel.²⁶ Despite a trend in the vertical loss in height, there was not a statistically significant change in the vertical height between the resin treated enamel and untreated adjacent tooth surface. These were promising results, which may be indicative of the stability of the resin infiltrant and its resistance to structural breakdown over time when subjected to repetitive mechanical abrasion.

Resin infiltration treatment for human teeth, if shown to exhibit resistance to toothbrush wear over time, may offer clinicians a promising tool in the management of post-orthodontic WSLs. Since the success of the resin infiltrant depends on its structural integrity, it is of interest to investigate Icon's® resistance to mechanical wear using a model similar to toothbrushing. Therefore, the purpose of the current study was to evaluate, using scanning electron microscopy (SEM), the microstructural changes of resin infiltrant after six months of simulated

toothbrushing in extracted human teeth. The null hypothesis was that there would be no visually detectable changes in microstructural surface characteristics on the infiltrative resin surface after six months of simulated toothbrushing.

Materials and Methods

In this *in vitro* study, previously extracted non-carious human third molars (n=10) were retrieved from the oral and maxillofacial surgery department. Teeth with no visible defects or demineralization were cleaned to remove any debris, and stored in 5% chloramine T hydrate solution (Fischer Chemical, Hampton, NH) for disinfection. The teeth were then transferred into vials filled with distilled water, and stored until the demineralization procedures were started. The most flat surface of each tooth was painted with a thin layer of an acid-resistant varnish (Revlon, Cherries in the Snow, New York City, New York) leaving a 3mm diameter circle in the middle of the crown surface exposed to the acidic solution.

The acidic solution was prepared according to the protocol outlined by Kumar et al.²⁷ by mixing 2.2 mM calcium chloride (Fisher Bioreagents, Hampton, NH), 0.05 mM acetic acid (Fisher Bioreagents, Hampton, NH), 2.2 mM monopotassium phosphate (EMD Millipore, Billerica, MA) and titrating the contents to a pH of 4.4 with 1.0 M potassium hydroxide (Fisher Chemical, Hampton, NH). A small hole was drilled near the apex of each tooth so that a non-fluoridated dental floss could be used to suspend teeth in the acidic solution. Samples were kept in the demineralizing medium for 10 days. Each day, the acidity of the solution was checked with a pH meter to ensure the solution was stable at or near 4.4 pH, and the tooth surfaces were examined for the development of white spot lesions (Figure 1).



Figure 1: Confirmation of WSLs on Pilot Teeth.

Following visual confirmation of the artificial WSLs, resin infiltrant was applied by the same operator to the demineralized area created within the 3mm diameter circle according to the manufacturer's instructions using the following steps:

1. 15% HCl acid gel application for 2 minutes while gently rubbing the gel to ensure the fresh etch contacted with the tooth surface.
2. Rinsing for 30 seconds with water followed by drying with oil free air.
3. Application of Icon Dry ethanol solution for 30 seconds, followed by oil free air drying.
4. Application of Icon Infiltrant, allowed to sit for 3 minutes. Removal of the excess resin with a cotton roll followed by light curing for 40 seconds
5. Application of Icon Infiltrant a second time, allowed to sit for 1 minute. Removal of the excess resin with a cotton roll followed by light curing for 40 seconds.
6. Polishing with fine and extra fine aluminum oxide polishing strips (Soflex, 3M ESPE, St Paul, MN)

Following the application of the resin infiltrant, four indentations were made at the north, east, west and south aspects of the circle using a number 8-round bur for easy identification of the resin treated surfaces under the microscope.

For the SEM analyses, tooth surfaces were examined using SEM under variable pressure, with values ranging between 40-70 Pa (Zeiss EVO-50XVP). The initial SEM analyses included the examination of tooth surfaces to establish the characteristics of the sound and demineralized enamel (n = 2, each). Microscopic images of the representative areas were taken at 250X magnification on each tooth surface. These micrographs provided the microscopic characteristics of sound and demineralized enamel surfaces, and later were used for comparisons between the baseline and follow-up images.

The resin treated tooth surfaces were first examined under the SEM at T1 which represented the original resin treated enamel. Images for each tooth were taken at 250X magnification, taken at three randomly selected points within the circular window. Following the initial analyses of the tooth surfaces for roughness, cracks and scratches, all samples were then subjected to the equivalent of 6 months of toothbrushing using a simulator (Figure 2).

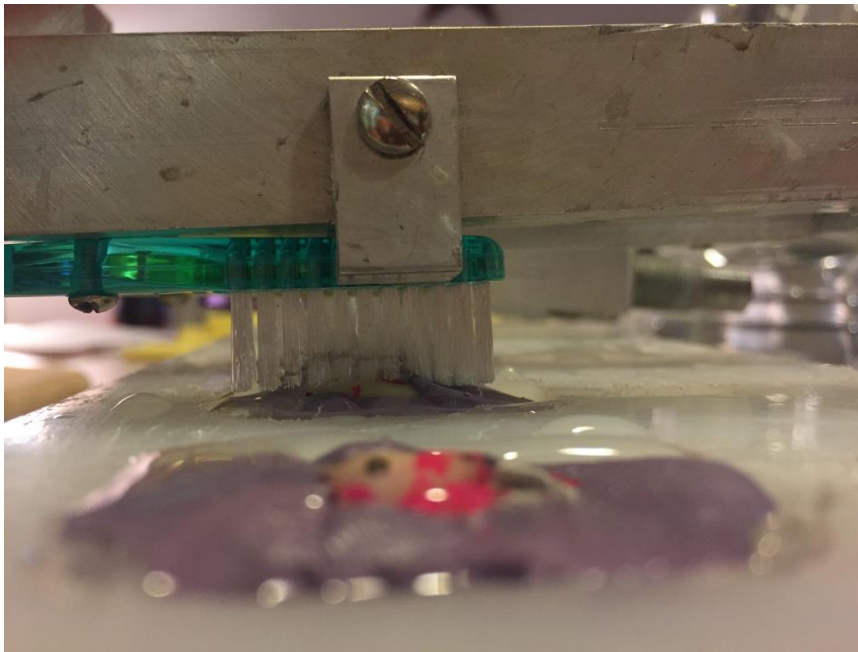


Figure 2: Mounting of tooth under toothbrush simulator.

In this study, a total of 2,500 horizontal strokes were applied to tooth surfaces to simulate six months of toothbrushing, assuming teeth were brushed two times per day for two minutes. The number of strokes were calculated based on the knowledge that, over the course of a two-year period and brushing three times per day, 15,000 toothbrush strokes on average are applied to each tooth in the human mouth.²⁸ Standard soft bristle toothbrushes (GUM 407 model, Sunstar Global, Schaumburg, IL) were mounted within the toothbrush simulator over one of the six wells. The teeth were mounted in separate wells within the simulator with the Icon-coated surface facing perpendicular to the toothbrush head and bristle tufts. The force of the toothbrush simulator was adjusted to apply 225 g of force during toothbrushing. Between measurements and experimental steps, teeth were stored in randomly numbered containers, submerged in room-temperature distilled water to prevent desiccation. All teeth were brushed using a fresh toothbrush to protect against wear of the bristles. A new toothbrush was also used after the equivalent of three months of toothbrushing. After toothbrushing, all teeth were again examined with variable pressure SEM using the same magnification parameters, defined as T2.

Two examiners were blinded to the images and time points and evaluated changes in images before and after toothbrushing for the presence of 1) enamel rods, 2) microcracks, and 3) fractures. For the purpose of grading the images, the presence of these characteristics was defined as present (Y) if more than 75% of the tooth surface imaged showed the presence of these features, partial (P) if between 25 and 75%, and absent (N) if viewed on less than 25% of the imaged tooth surface. A total of 60 SEM images, 30 at each timepoint, were evaluated by two examiners (Appendix I). Inter-rater reliability was tested for using Cohen's Kappa, and changes between T1 and T2 were compared across time using Bowker's test for symmetry for a single rater's evaluations. Additionally, association between presence of enamel rods with both

microcracks and fissures were tested using a chi-squared test. A significance level of $p = 0.05$, and program SAS EG v6.1 were used for all statistical analyses.

Inter-rater correlation was classified as strong for scored images at 250X magnification for presence (Y), partial (P), or absence (N) of enamel rods ($\kappa=0.80$), microcracks ($\kappa=0.80$), and fractures ($\kappa=0.81$).

Results

All of the resin-treated tooth surfaces had, to some degree, microstructural features consisting of enamel rods, microporosity, fissures, and cracks.

Enamel rods were generally present both in the sound enamel and enamel treated with infiltrative resin, and in both samples were approximately 4 microns in diameter. This was consistent with measurements found in previous studies which showed the diameter of enamel prisms averaging 4 to 5 microns, with a cylindrical appearance.²⁹ However, in the demineralized samples, increased porosity was noted at the surface with dissolution of the prism core and thus a larger diameter in width of the rod at the periphery, with many as wide as 6 or 7 microns (Figures 3 and 4).

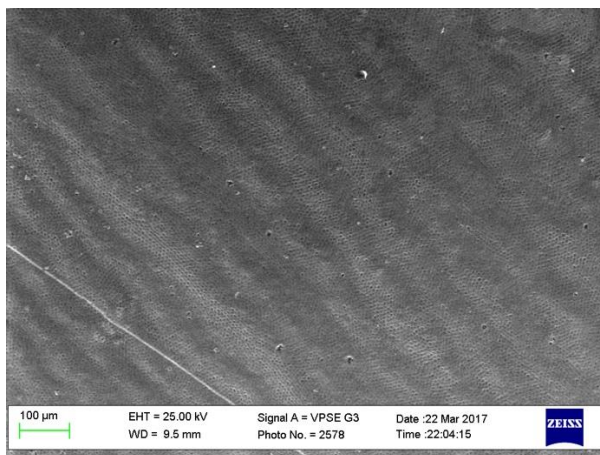


Figure 3: Baseline Image of Sound Enamel. Tooth B. 250X Magnification.

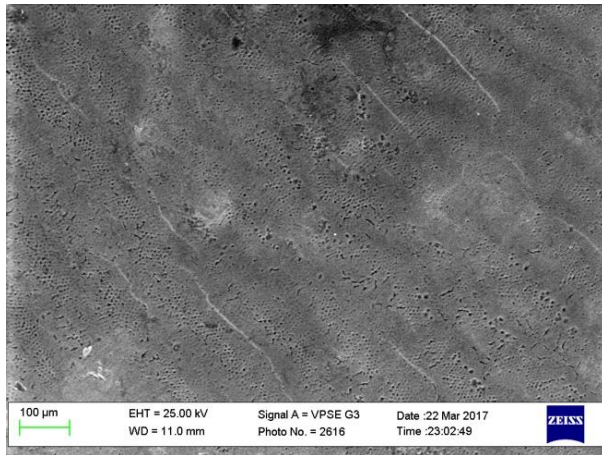


Figure 4: Baseline Image of Demineralized Enamel. Tooth C. 250X Magnification.

This increased porous enamel was successfully infiltrated in the experimental teeth, which was determined by the absence of hollow prism cores and a restoration of an intact surface. A common presentation of the samples included areas of concentrated enamel rods visible at the level of the tooth surface, with resin either displaying a slight thickness which was visible on the tooth surface in irregular patterns, or interspersed within the typical honey-comb pattern of the enamel rods, filling in areas of porosity between adjacent prisms. While significant heterogeneity existed between teeth, visualization of enamel rods within the resin, as well as microcracks, and fissures, in varying degrees, were common findings. While the porosities in the demineralized tooth structure appeared successfully infiltrated, returning its surface appearance closer to that of sound enamel, the resin coated surfaces did maintain a high degree of visible roughness and surface irregularity. SEM images from T2 appeared generally similar to those in T1, and qualitative differences before and after toothbrushing were mainly noted by direct comparison of paired images. Characteristic images are shown from teeth prior to toothbrushing below (Figures 5-7).

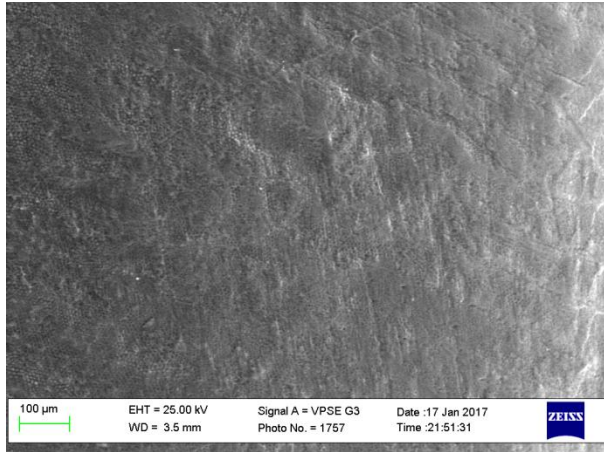


Figure 5: Tooth 2. Location B. T1. 250X Magnification.

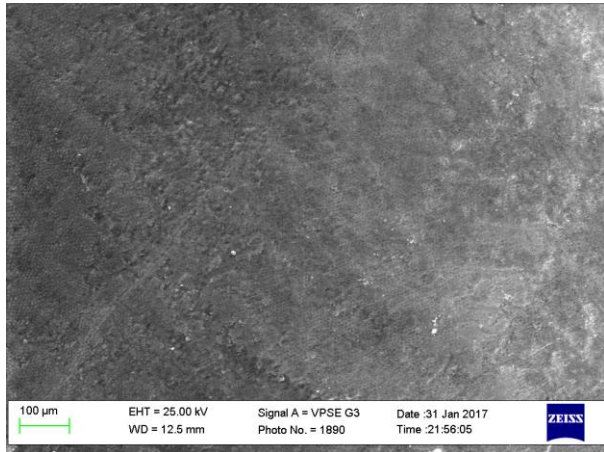


Figure 6: Tooth 4. Location B. T1. 250X Magnification.

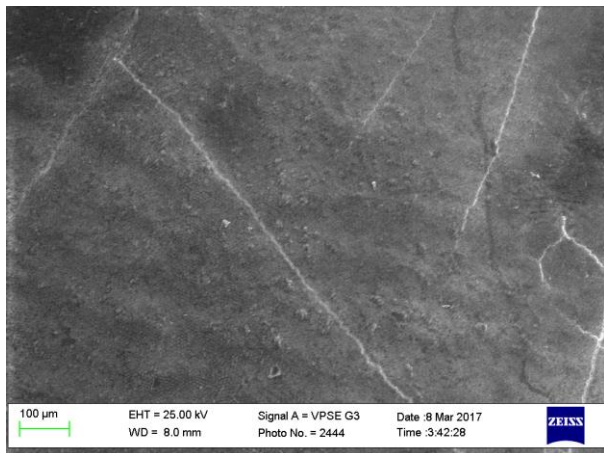


Figure 7: Tooth 10. Location B. T1. 250X Magnification.

Changes in the presence of enamel rods, microcracks, or fractures between time points are illustrated in Figures 8-10. While some qualitative changes were noted on paired images over time, none of the overall changes in presence of these microstructural characteristics were found to be statistically significant ($p = 0.4753$, $p = 0.3618$, and 0.3916 , respectively). Table 1 displays the total number of teeth present within each category before and after toothbrushing, as well as the total percentage of paired images which showed a change in characterization between time points.

Table 1: Distribution of SEM Characterizations between T1 and T2.

	Enamel Rods		Fractures		Microcracks	
	T1	T2	T1	T2	T1	T2
Y	15, 50%	17, 57%	6, 20%	9, 30%	7, 23%	10, 33%
P	9, 30%	5, 17%	8, 27%	4, 13%	12, 40%	13, 43%
N	6, 20%	8, 27%	16, 53%	17, 57%	11, 37%	7, 23%
Total Changed	10, 33%		14, 47%		11, 37%	

Figure 8 shows into which specific categories the movement was evident between paired images for presence of enamel rods. At T1, 15 SEM images were found to have enamel rods present (Y), 9 images had enamel rods partially present (P), and 6 showed an absence of enamel rods (N). After toothbrushing, 33% of the images were characterized into different groups than they were at T1 for presence of enamel rods, indicative of some surface changes occurring. Of the images initially showing a presence of enamel rods, a majority (80%) of these teeth were still found to show presence of rods after toothbrushing. None of the images which showed absence of enamel rods were found at T2 to have exposure of enamel rods which would result in movement into either the partial or the present categories. While it was evident that change occurred between time points in the images, the net changes over time of presence of enamel rods was not statistically significant, with most of the changes occurring in the teeth which were described as having partial enamel rod coverage prior toothbrushing ($p = 0.4753$).

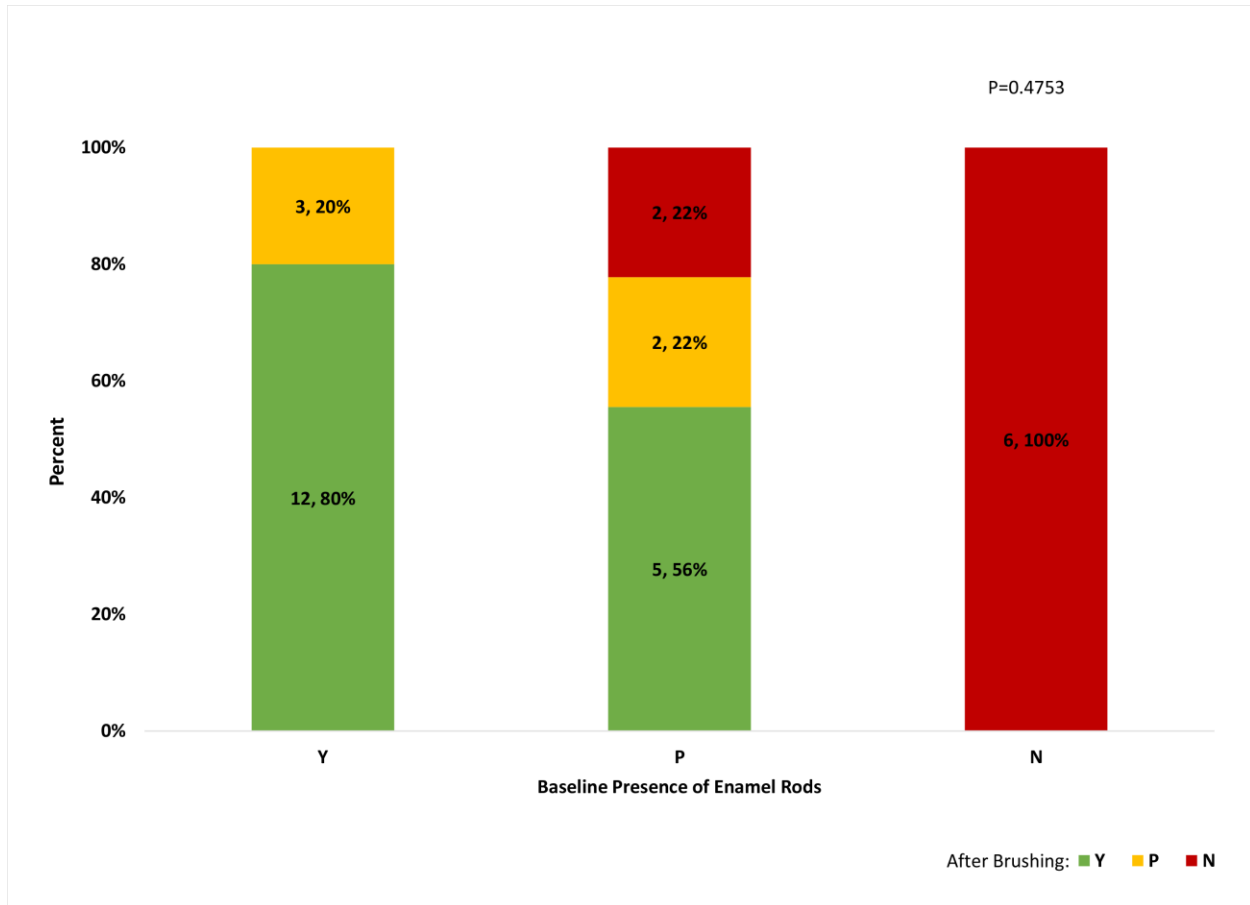


Figure 8: Changes in Presence of Enamel Rods After Simulated Brushing.

Microcracks and fissures present on the resin surface were common findings throughout the samples. For this study, fractures were defined as fissures within the resin-enamel interface where a cleft-like gap could be visually detected at 250X magnification. Microcracks displayed a similar appearance to fractures, however the surface of the resin appeared intact, without gap formation. Figure 9 displays the distribution of all samples regarding microcracks at the surface before and after toothbrushing. At T1, 63% of the images displayed microcracks present at some level (either present or partially present), and 37% of the images had a change in classification after toothbrushing. Of images which were found to have presence (Y) of microcracks at T1, 71% of these images were still found to have microcracks after toothbrushing, and no pair of

images evaluated showed enough of a decrease in microcracks to be defined as absent of this characteristic. Twelve images were found to have partial occurrence of microcracks at baseline. Of these images, 25% of the images were judged to have more microcracks uncovered at T2, and 8% had removal of microcracks from the surface. Similar to the changes in enamel rods, while changes in the distribution of microcracks did occur between groups, these differences were not found at a level of statistical significance to result in a predictable change in any particular direction ($p = 0.3618$).

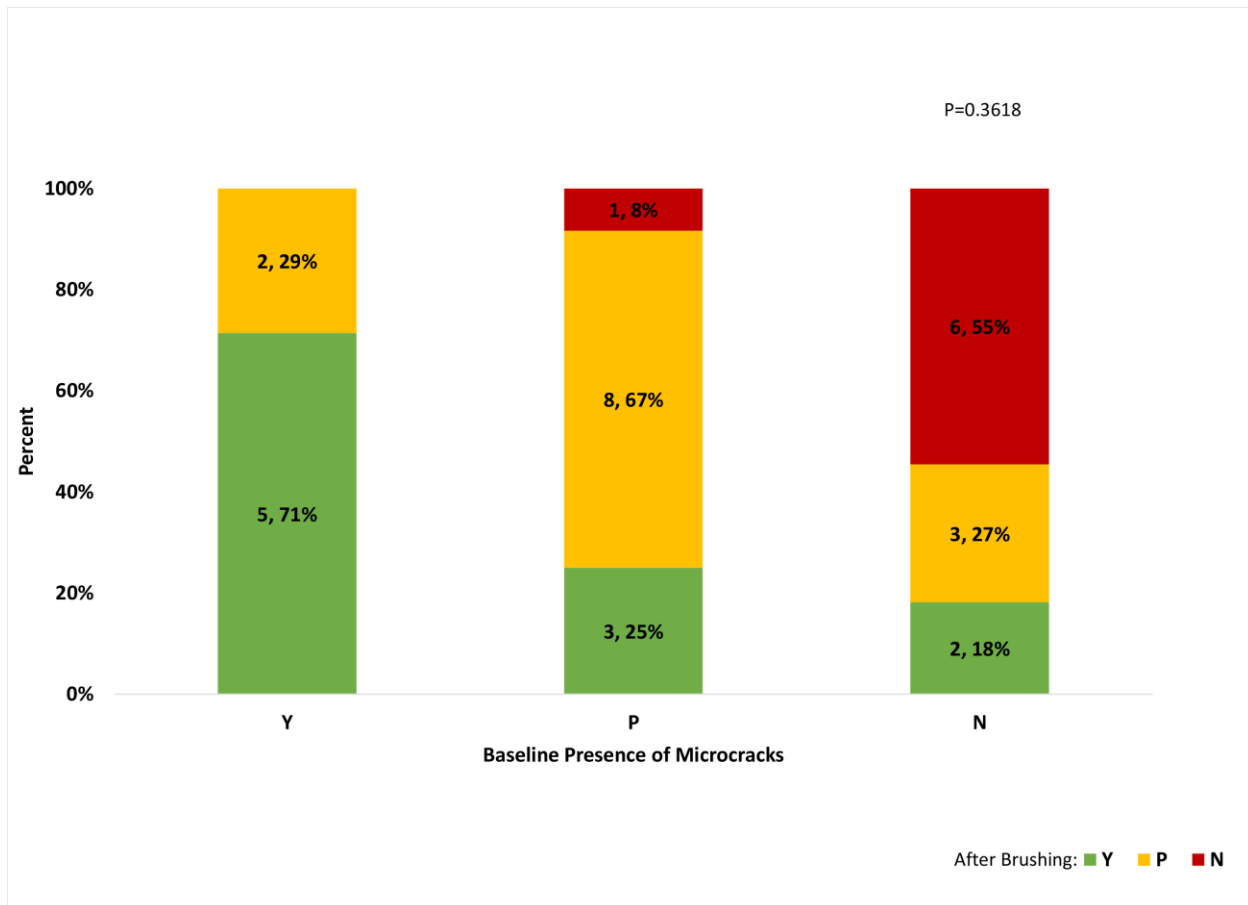


Figure 9: Changes in Presence of Microcracks After Simulated Brushing.

Fractures were found to be present on 6 of the tooth images at T1, partially present on 8

images, and absent on 16 images at T1. In other words, 47% of the tooth images showed gap formation severe enough at the surface of the resin to be able to visualize a cleft-like fissure within the resin. Interestingly, just under half (47%) of these teeth had a change in characterization from before to after toothbrushing, with most of the change evident within the present and partially present groups. For example, of the teeth with fractures present at T1, 50% were still present after toothbrushing, and 33% of images showed fractures only partially present. When fissures were not present at T1, 75% of the teeth continued to show absence of fissures after brushing (Figure 10). Again, despite changes in the characterization of 47% of images regarding fractures, there was not a statistically significant difference for fracture presence to change in either a positive direction (more fractures over time) or negative direction (less fractures over time) ($p=0.3916$).

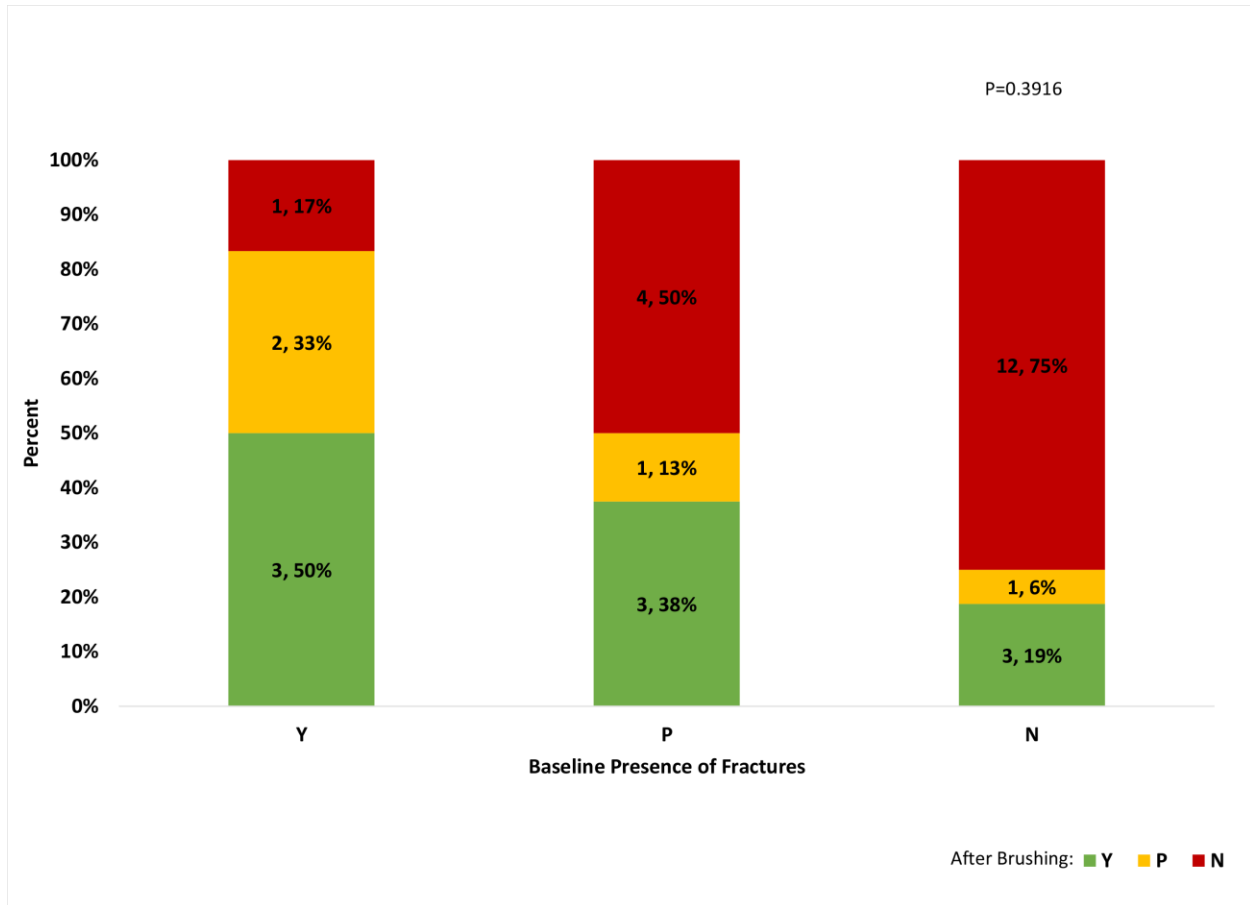


Figure 10: Changes in Presence of Fractures After Simulated Brushing.

Of additional interest was the association between presence of enamel rods and both microcracks and fractures. There was a significant positive correlation between absence of enamel rods and presentation of both microcracks ($p = 0.0009$) and fractures ($p = 0.0021$). Specifically, of the images which did not display a presence of enamel rods, 71% of these images also displayed microcracks and 36% displayed fractures. Figures 11 and 12 depict these relationships below.

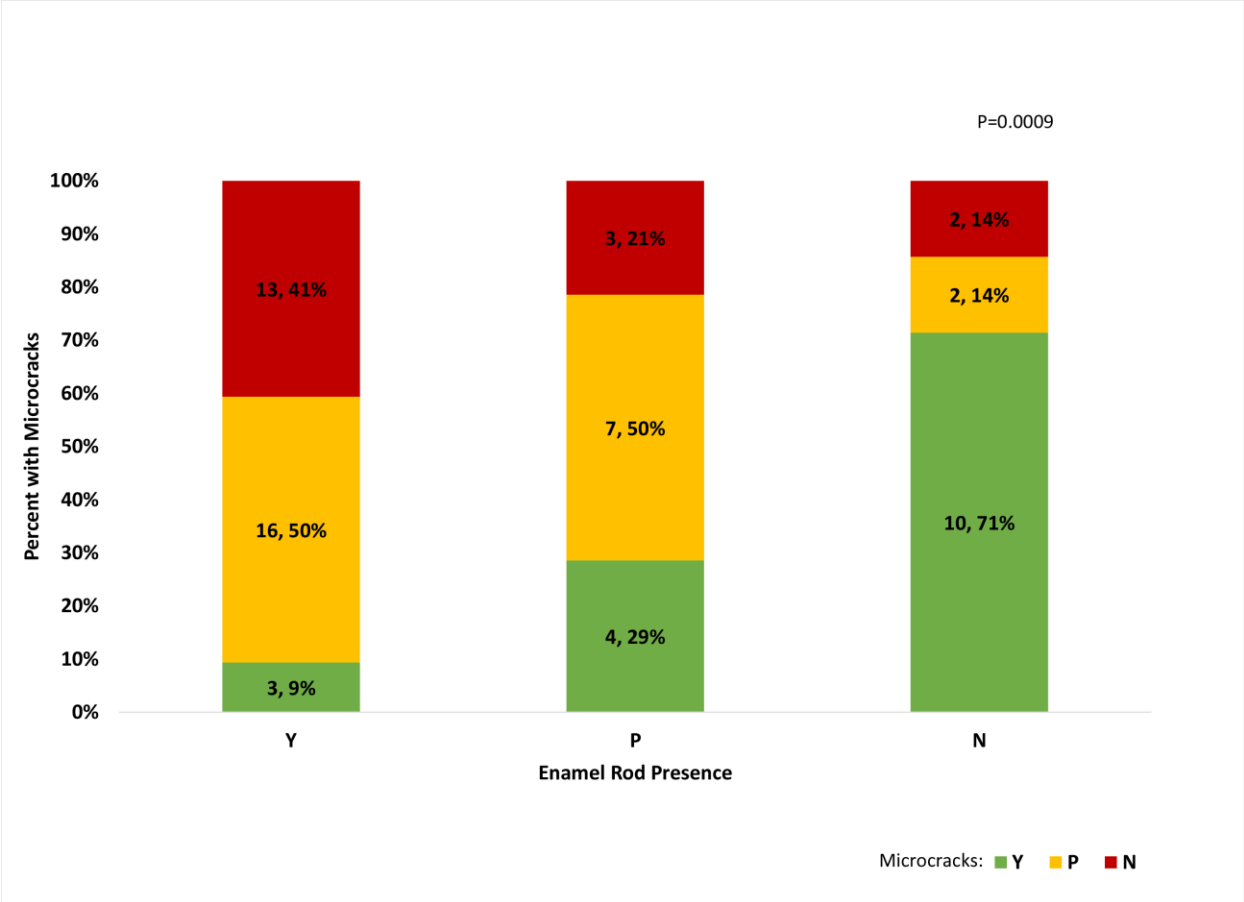


Figure 11: Association between Enamel Rods and Microcracks

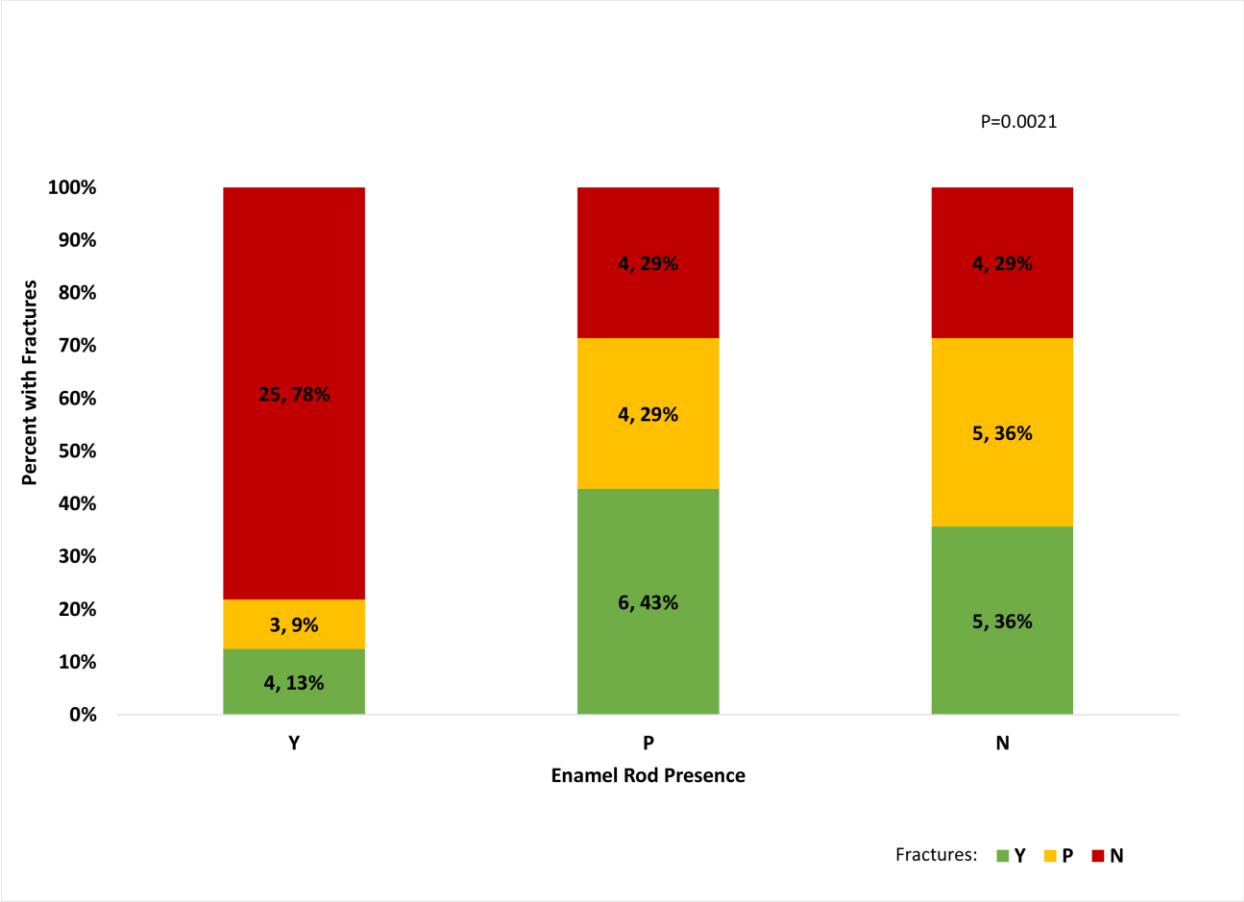


Figure 12: Association between Enamel Rods and Fractures

Discussion

While small changes in microstructural characteristics were noted qualitatively in infiltrative resin treated tooth surfaces, none of these differences were large enough in this study's sample to result in statistical significance. Therefore, it may be concluded that there were not significant changes in the microstructural characteristics of resin infiltrant after six months of simulated toothbrushing. However, some qualitative changes were observed which should be taken into consideration for the clinical use of infiltrative resin treatment for WSLs.

Infiltrative resin, compared to other resins, sealants, or composites, is uniquely difficult to detect with the naked eye due to its nature as a colorless resin, which takes on the color of the sound enamel which it infiltrates. Thus, changes in fluorescence or differences in color are not reliable methods to detect its presence as it can be with other resin materials. Even microscopically, the resin was found to restore the appearance of demineralized enamel back to that close to the appearance of sound enamel, and at times detection between infiltrated enamel and sound enamel alone was challenging.

A high degree of roughness of the infiltrative resin surface was noted throughout samples. This is consistent with previous studies which have shown that after application of infiltrative resin, the roughness of the infiltrated teeth even approximates that of demineralized enamel.^{30,31} This finding of significant roughness was also found in the current study. As is visible in the comparison below, small scratches after polishing, despite polishing with "fine" and "very fine" aluminum-oxide coated polishing discs, are present at 250X magnification

(Figure 13). These areas of roughness were noted in many instances to be smoothed by six months of simulated toothbrushing. Comparing T2 at this same location on this tooth, it can be noted that, while resin is still apparent, the number of surface scratches decreased. However, microcracking is seen toward the right side of the image indicating the resin is present at the surface, as well as still interspersed between the enamel rods throughout the image.

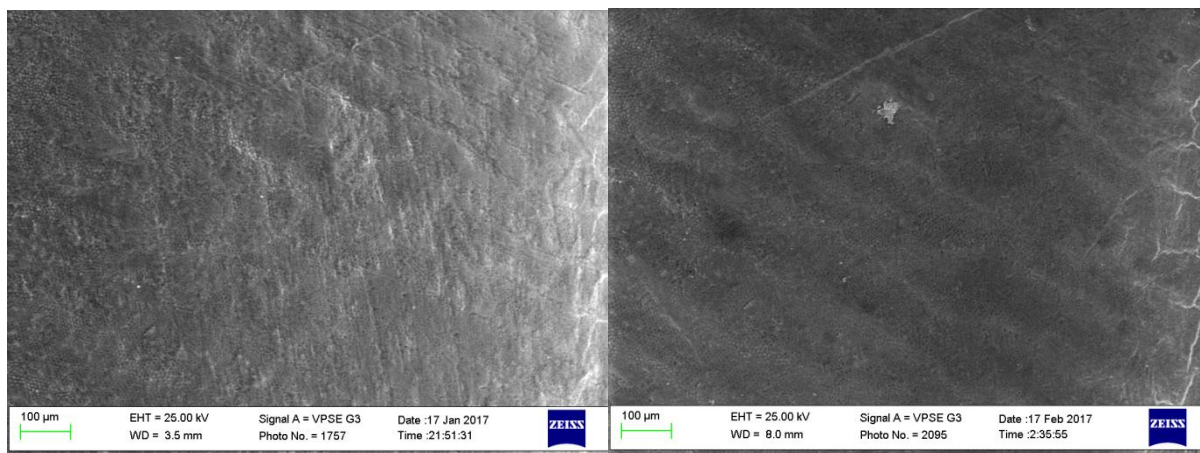


Figure 13: Tooth 2. Location B. T1 (left) and T2 (right). 250X Magnification.

Another feature, which was found in some samples across time, was the opening of fractures at the resin-enamel surface after toothbrushing. A frequent presentation was that microcracks identified before toothbrushing changed appearance to that of a fracture after toothbrushing. While this phenomenon did not occur with high enough frequency to show statistical significance in this study's sample, it should be noted that the manufacturer of Icon® recommends a second application of resin to fill in potential gaps that could form due to polymerization shrinkage.^{16,17} The change from a microcrack to a fracture is indicative that a small surface layer of infiltrative resin, which may have been occluding these fractures, was removed by toothbrushing, re-exposing the gap within the resin. The comparison between T1 and T2 below on one sample (Figure 14) shows a dramatic representation of this phenomenon.

Since gap formation at the enamel-resin interface may be susceptible to bacterial, acid, or mechanical attack, repeated application of resin infiltrant six months after initial application could be useful to prevent leakage in these areas of wear.¹⁵

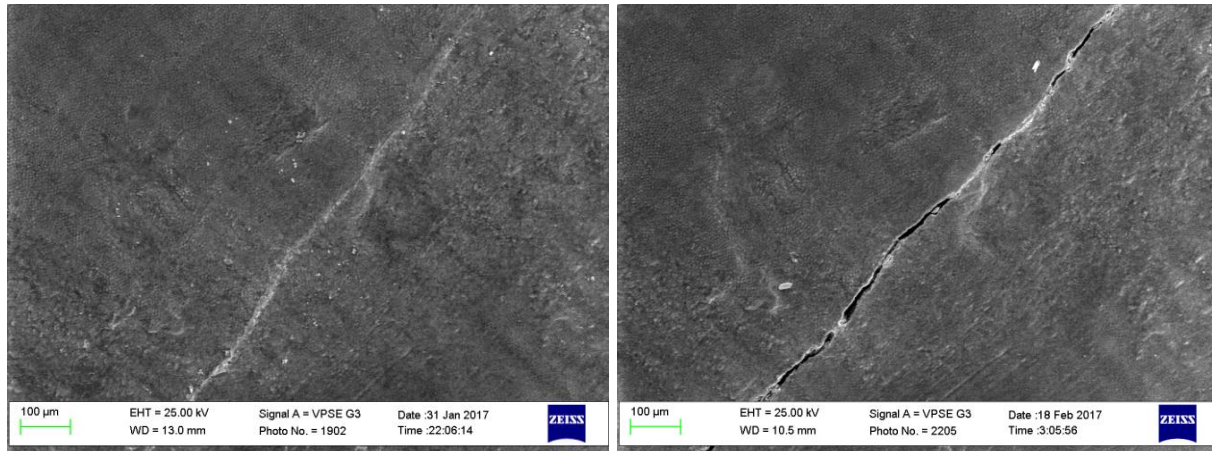


Figure 14: Comparison between T1 (left) and T2 (right) of Tooth 4. Location C. 250X Magnification.

It should also be noted that not all teeth with microcracks became fissured after toothbrushing. In some instances, brushing the tooth surface either removed or lessened the quantity of microcracks, and in other cases uncovered new sub-surface microcracks. It is important to note that any movement between categories in the current study was indicative of a surface change. Even if there wasn't a statistically significant pattern to these changes, their overall presence indicates potentially significant clinically changes. Removal or uncovering of additional microcracks and fractures indicates that some qualitative changes in the surface characteristics of the resin took place. This was also true in the case of enamel rod presentation.

One of the most striking findings in the current study was the high degree of heterogeneity between the appearances of all the images. Several different explanations for these differences can be hypothesized, including: 1) Embedded debris or contaminants may have

altered the surface appearance. Specifically, removal of the excess surface layer by cotton rolls could have left small cotton fibers in the surface layer of resin. 2) Differences in natural tooth anatomy may explain why some teeth showed higher prevalence of features such as craze lines. 3) Some teeth may have displayed more fracturing from traumatic extraction procedures. 4) Perhaps some teeth experienced more fracturing from desiccation during the sample preparation for SEM analysis than others. Many of these causes of heterogeneity between samples are also proposed reasons why many of the images show significant surface roughness.

An additional important finding of the current study was the significant correlation between absence of enamel rods visible at the tooth surface and an increase in the presence of microcracks and fissures ($p = 0.0009$, and $p = 0.0021$, respectively). These were specimens in which a thicker layer of resin appeared to be present at the surface. Previous studies have shown that when resin is present in an increased thickness, the internal pressure from polymerization shrinkage is in turn significantly increased.^{16,17,32} As a result, higher gap formation and fracturing is often found within the enamel-resin layer. While removal of the surface layer of resin with a cotton roll prior to polymerization is recommended, it may be tempting for some practitioners to want to leave this excess in place as a potential layer of sealant. The results of this study indicate that this practice could be contraindicated, and lead to decreased structural integrity of the resin. However, this should be weighed against the extra protective benefit previous studies have shown, that leaving an excess of resin on the surface could protect the teeth against acid erosion.³³ Figures 15-17 show instances of higher resin fracturing when enamel rods are not present, and the surface-resin layer appears thickened.

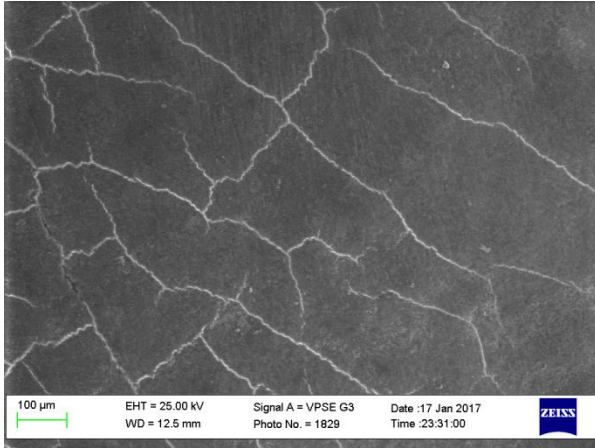


Figure 15: Tooth 1. Location B. T1. 250X Magnification.

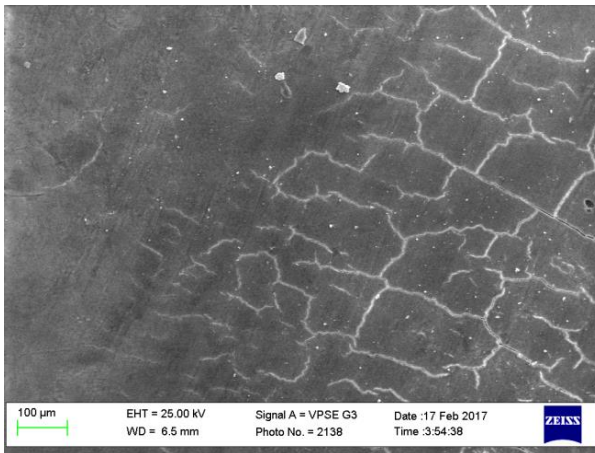


Figure 16: Tooth 3. Location B. T2. 250X Magnification.

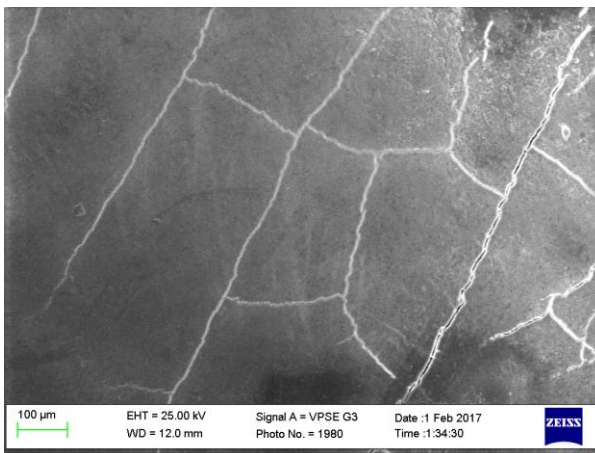


Figure 17: Tooth 6. Location B. T1. 250X Magnification.

Studies have also shown an increased tendency for infiltrative resin to stain over time.²¹⁻²⁴ The roughness, microcracks, and fractures found at the surface of the teeth offer possible explanations for why the staining occurs. Rougher surfaces provide more areas for highly staining pigments to leak into and/or become trapped within.³⁴ Polishing would thus remove the discoloration, as was corroborated by the results of the study by Leland et al.,²⁴ where esthetics was improved when staining from coffee and wine were eliminated by pumice polishing of the tooth surface.

In this study, the use of variable pressure SEM as a microscopic technique allowed for evaluation of the infiltrative resin with minimal manipulation or alteration at the tooth surface. SEM with variable pressure enables imaging of non-conductive material such as teeth by lowering the pressure within the gas chamber until artefacts created from electron charging are no longer present, thus eliminating the need for a conductive coating. This technique is particularly useful for biological samples as they can be viewed in their natural state, without the addition of a conductive material coating added to the surface as is typical with conventional SEM.

One of the compromises of using a variable pressure SEM, however, is the possibility of artefact creation from contamination of images with material of higher or lower conductive potential than the material of interest. While contamination was generally not found to be present in the samples, there were a few isolated images where this was noted as areas of either excessively light or dark streaks of unknown material. Additionally, while low vacuum imaging is not quite as high in resolution as conventional SEM, it was found to be sufficient for the current study to achieve high quality imaging at 250X.

An additional unavoidable limitation of variable pressure SEM is the time required outside of liquid. All teeth in the study required mounting on pegs for placement within the imaging chamber, and since variable pressure SEM is a slower microscopy technique, this can result in high degrees of desiccation of samples. While teeth in the samples were stored in distilled water between all other experimental steps, it is possible that changes in the surface structure could have occurred during the time required for imaging. Specifically, enamel has a higher modulus of elasticity than dentin, and thus when dentin desiccation and shrinkage occurs, the fragile enamel prisms are sometimes found to crack at the enamel surface from tensile stresses.^{32,35} Because some microcracks were found to be present on the surfaces of baseline teeth A-D (although typically in smaller numbers), this was taken into consideration as a possible etiology of enamel microcracks in all images.

A recent study by Arnold et al.³¹ investigated the effects of 15% HCl on enamel. Over a course of 2 minutes, this etchant was found to remove an average of 34 microns of enamel. Two rounds of two minutes of etching time, which is the recommended protocol for infiltrative resin, increased enamel removal further 13.28 microns. In vivo, the double etching is often necessary to remove the hardened outer layer of enamel which is created by salivary remineralization at the enamel surface.³⁶ However, since in our pilot study the double application of etchant resulted in complete removal of the WSL, in the current study the samples were subjected to only a single two-minute application of 15% HCl. While it could be argued that the etching process recommended for resin infiltration removes a significant layer of enamel in the process, Meyer-Lueckel et al.³⁶ noted that the procedure still removes far less enamel than other treatments such as veneers or microabrasion, which can remove as much as 360 microns of enamel.³¹

There were some limitations to note with the design of this study. The in-vitro creation of white spot lesions, storage conditions, and simulated “daily” challenges have inherent differences compared to teeth in vivo. For example, it is known that WSLs in vivo often tend to be deeper, more longstanding, and may have a hardened surface layer from remineralization in the oral environment, which can be difficult to remove with etching procedures.⁸⁻¹⁰ A recently published study by Zhao et al.³⁷ which investigated both the effect of toothbrush abrasion (600 strokes total) and acidic challenge with orange juice, found material loss via profilometry to average 24.6 microns. Furthermore, in that study the Icon® layer was shown to be completely removed with acid and mechanical abrasion. Thus, additional challenges such as acid and bacterial presence could cause differences in how infiltrative resin behaves over time.

Prior studies investigating the extent of demineralization have shown a wide range in depth of infiltration by TEGDMA based infiltrative resins, from 15.7 microns to over 400 microns in others in vitro.^{37,38} Belli et al.²⁶ investigated vertical loss of infiltrated enamel in bovine teeth, and found an average loss of 42.6 microns of resin-enamel structure following 20,000 toothbrush abrasion cycles. Evaluating the depth of penetration would not have been feasible in this SEM study, since sectioning of the samples would be required to evaluate depth penetration. In this case, it would not have been possible to evaluate the tooth surfaces at the second time point of the toothbrushing simulation procedures.

Ideally, atomic force microscopy to measure microscopic surface roughness and/or a Vicker’s hardness test would have been useful additional quantitative information to characterize the behavior of Icon® over time. However, both of these methods would require a virtually flat surface to be accurate. It is possible that flat enamel discs could be created for infiltrative resin application; however, this preparation would require removal of the surface layer of enamel,

which is typically found to be more fluoride-rich than the underneath layers due to presence of fluoride available in the mouth. Therefore, it should be kept in mind that enamel prepared into a slab may behave differently than enamel on the natural tooth surfaces.

To date, this is the first study to fully evaluate the microstructural changes of an infiltrative resin applied to WSLs in human teeth over time when challenged with toothbrush abrasion. Future studies with larger sample size, longer duration and conditions more closely approximating that of the natural oral environment are needed to investigate the cause of enamel-resin gap formation after resin application and the wear of this material over time.

Conclusions

- 1) After six months of simulated toothbrushing on enamel surfaces with WSLs coated with resin infiltrate, there were microstructural changes in enamel rods, microcracks, and fractures, but overall differences were not statistically significant.
- 2) An increase in incidence of fractures and microcracks was positively correlated with a thicker surface layer of resin infiltrate.
- 3) Failure to remove the residual surface layer of infiltrative resin prior to light-curing may result in higher fractures and gap formation within the resin due to polymerization shrinkage.
- 4) Due to the qualitative surface changes after 6 months of simulated toothbrushing, additional application of resin may be indicated over time.

Literature Cited

Literature Cited

- (1) Taher NM, Alkhamis HA, Dowaidi SM. The influence of resin infiltration system on enamel microhardness and surface roughness: An in vitro study. *Saudi Dent J.* 2012;24(2):79-84.
- (2) Julien KC, Buschang PH, Campbell PM. Prevalence of white spot lesion formation during orthodontic treatment. *Angle Orthod.* 2013;83(4):641-647.
- (3) Tufekci E, Dixon JS, Gunsolley JC, Lindauer SJ. Prevalence of white spot lesions during orthodontic treatment with fixed appliances. *Angle Orthod.* 2011;81(2):206-10.
- (4) Gorelick L, Geiger AM, Gwinnet AJ. Incidence of white spot formation after bonding and banding. *Am J Orthod.* 1982;81:93-98.
- (5) Sundararaj D, Venkatachalapathy S, Tandon A, Pereira A. Critical evaluation of incidence and prevalence of white spot lesions during fixed orthodontic appliance treatment: A meta-analysis. *J of Int Soc of Prev Community Dent.* 2015;5(6):433-439.
- (6) Maxfield BJ, Hamdan AM, Tüfekçi E, Shroff B, Best AM, Lindauer SJ. Development of white spot lesions during orthodontic treatment: perceptions of patients, parents, orthodontists, and general dentists. *Am J Orthod Dentofacial Orthop.* 2012;141(3):337-344.
- (7) Griffin SO, Regnier E, Griffin PM, Huntley V. Effectiveness of fluoride in preventing caries in adults. *J Dent Res.* 2007;86(5):410-415.
- (8) Ogaard B, Rølla G, Arends J, ten Cate JM. Orthodontic appliances and enamel demineralization. Part 2. Prevention and treatment of lesions. *Am J Orth Dentofacial Orthop.* 1988;94(2):123-128.
- (9) Ogaard B. The cariostatic mechanism of fluoride. *Compend Contin Educ Dent.* 1999; 20(1 Suppl):10-7.
- (10) Zantner C, Martus P, Kielbassa AM. Clinical monitoring of the effect of fluorides on long-existing white spot lesions. *Acta Odontol Scandinavica.* 2006;64(2):115-122.
- (11) Senestraro SV, Crowe JJ, Wang M, Vo A, Huang G, Ferracane J, Covell DA Jr. Minimally invasive resin infiltration of arrested white-spot lesions: a randomized clinical trial. *J Am Dent Assoc.* 2013;144(9):997-1005.

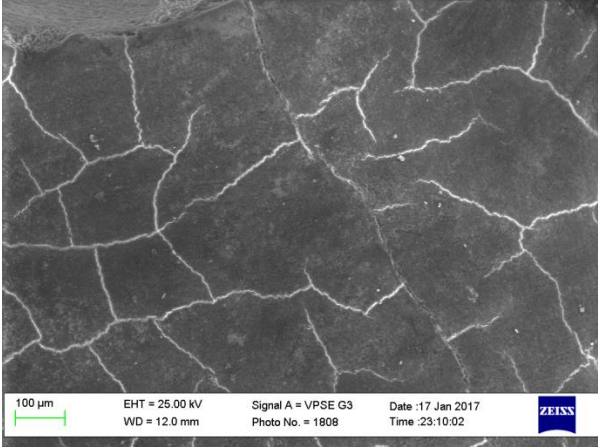
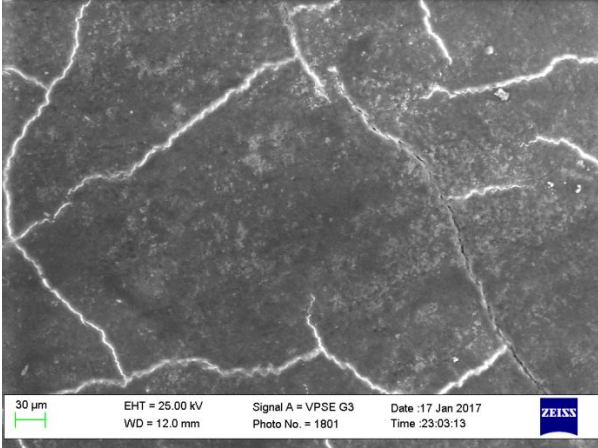
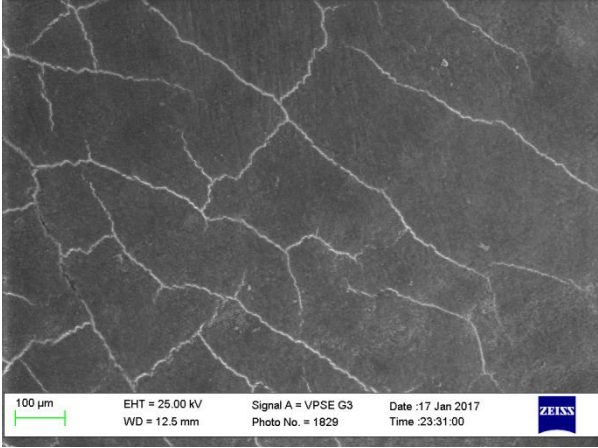
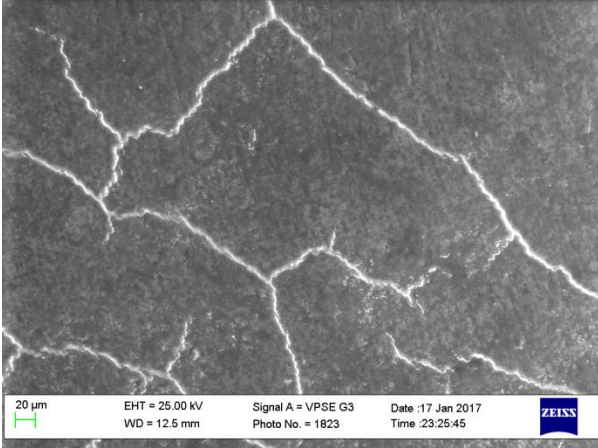
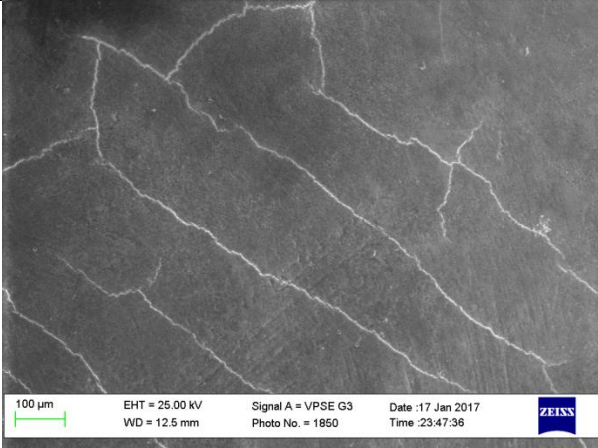
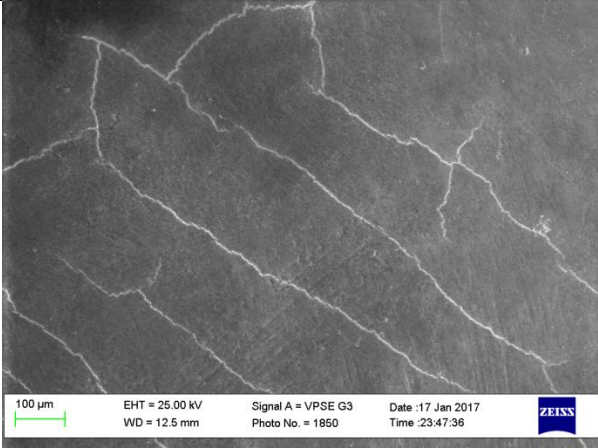
- (12) Borges AB, Caneppele TMF, Masterson D, Maia LC. Is resin infiltration an effective esthetic treatment for enamel development defects and white spot lesions? A systematic review. *J Dent*. 2017 56(1):11-18.
- (13) Arnold WH, Gaengler P. Light- and electronmicroscopic study of infiltration of resin into initial caries lesions - a new methodological approach. *J Microsc*. 2011;245(1):26-33.
- (14) Askar H, Lausch J, Dörfer CE, Meyer-Lueckel H, Paris S. Penetration of micro-filled infiltrant resins into artificial caries lesions. *J Dent*. 2015;43(7):832-838.
- (15) Paris S, Meyer-Lueckel H. Inhibition of caries progression by resin infiltration in situ. *Caries Res*. 2010;44(1):47-54.
- (16) Paris S, Meyer-Leuckel H, Colfen H, Kielbassa AM. Resin infiltration of artificial enamel caries lesions with experimental light curing resins. *Dent Mater J*. 2007;26(4):582-588.
- (17) Robinson C, Brookes SJ, Kirkham J, Wood SR, Shore RC. In vitro studies of the penetration of adhesive resins into artificial caries-like lesions. *Caries Res*. 2001;35(2):136-141.
- (18) Paris S, Schwendicke F, Seddig S, Müller WD, Dörfer C, Meyer-Lueckel H. Micro-hardness and mineral loss of enamel lesions after infiltration with various resins: influence of infiltrant composition and application frequency in vitro. *J Dent*. 2013;41(6):543-548.
- (19) Van Meerbeek B, Willems G, Celis JP, Roos JR, Braem M, Lambrechts P, Vanherle G. Assessment by nano-indentation of the hardness and elasticity of the resin-dentin bonding area. *J Dent Res*. 1993;72(10):1434-1442.
- (20) Watts DC, McNaughton V, Grant AA. The development of surface hardness in visible light-cured posterior composites. *J Dent*. 1986;14(4):169-174.
- (21) Araújo G, Naufel FS, Alonso RC, Lima DA, Puppim-Rontani RM. Influence of Staining Solution and Bleaching on Color Stability of Resin Used for Caries Infiltration. *Oper Dent*. 2015;40(6):E250-6.
- (22) Borges A, Caneppele T, Luz M, Pucci C, Torres C. Color stability of resin used for caries infiltration after exposure to different staining solutions. *Oper Dent*. 2014;39(4):433-440.
- (23) Cohen-Carneiro F, Pascareli AM, Christino MR, Vale HF, Pontes DG. Color stability of carious incipient lesions located in enamel and treated with resin infiltration or remineralization. *Int J Paediatric Dent*. 2014;24(4):277-285.
- (24) Leland A, Akyalcin S, English JD, Tufekci E, Paravina R. Evaluation of staining and color changes of a resin infiltration system. *Angle Orthod*. 2016; 86(6):900-904.

- (25) Yetkiner E, Wegehaupt FJ, Attin R, Wiegand A, Attin T. Stability of two resin combinations used as sealants against toothbrush abrasion and acid challenge in vitro. *Acta Odontol Scand.* 2014;72(8):825-830.
- (26) Belli R, Rahiotis C, Schubert EW, Baratieri LN, Petschelt A, Lohbauer U. Wear and morphology of infiltrated white spot lesions. *J Dent.* 2011;39(5):376-385.
- (27) Kumar VL, Itthagarun A, King NM. The effect of casein phosphopeptide-amorphous calcium phosphate on remineralization of artificial caries-like lesions: An *in vitro* study. *Aust Dent J.* 2008;53:34-40.
- (28) Hu W, Featherstone JD. Prevention of enamel demineralization: an in-vitro study using light-cured filled sealant. *Am J Orthod Dentofacial Orthop.* 2005;128(5):592-600.
- (29) Xie ZH, Mahoney EK, Kilpatrick NM, Swain MV, Hoffman M. On the structure-property relationship of sound and hypomineralized enamel. *Acta Biomaterial.* 2007;3(6):865-872.
- (30) Mueller J, Yang F, Neumann K, Kielbassa AM. Surface tridimensional topography analysis of materials and finishing procedures after resinous infiltration of subsurface bovine enamel lesions. *Quintessence Int.* 2011;42(2):135-47.
- (31) Arnold WH, Haddad B, Schaper K, Hagemann K, Lippold C, Danesh GH. Enamel surface alterations after repeated conditioning with HCl. *Head Face Med.* 2015;25(11):32.
- (32) Yoshikawa T, Morigami M, Sadr A, Tagami J. Environmental SEM and dye penetration observation on resin-tooth interface using different light curing method. *Dent Mater J.* 2016;35(1):89-96.
- (33) Tereza GP, de Oliveira GC, de Andrade Moreira Machado MA, de Oliveira TM, da Silva TC, Rios D. Influence of removing excess of resin-based materials applied to eroded enamel on the resistance to erosive challenge. *J Dent.* 2016;47(4):49-54.
- (34) Mair LH. Surface permeability and degradation of dental composites resulting from oral temperature changes. *Dent Mater.* 1989;5(4):247-255.
- (35) Ikeda T, Uno S, Tanaka T, Kawakami S, Komatsu H, & Sano H. Relation of enamel prism orientation to microtensile bond strength. *Am J Orthod Dentofacial Orthop.* 2002;15(2), 109-113.
- (36) Meyer-Lueckel H, Paris S, Kielbassa AM. Surface layer erosion of natural caries lesions with phosphoric and hydrochloric acid gels in preparation for resin infiltration. *Caries Res.* 2007;41(3):23-30.
- (37) Zhao, X., Pan, J., Zhang, S. et al. Effectiveness of resin-based materials against erosive and abrasive enamel wear. *Clin Oral Investig* 2017;21(1):463-468.

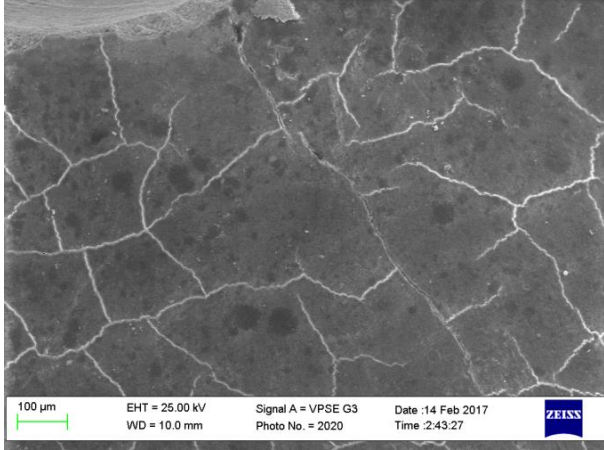
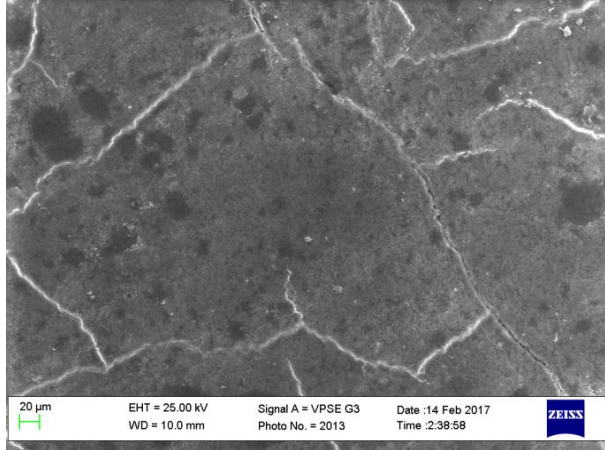

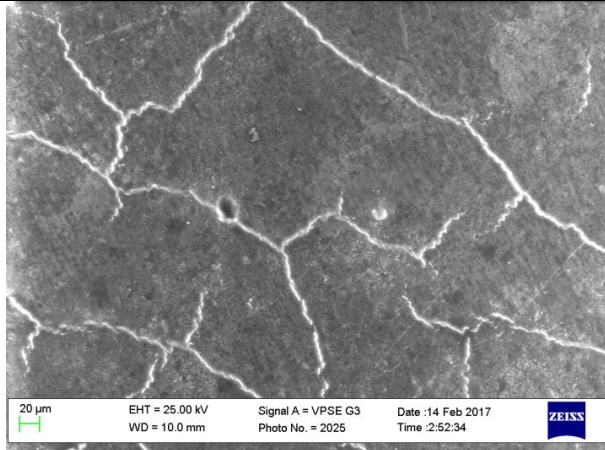
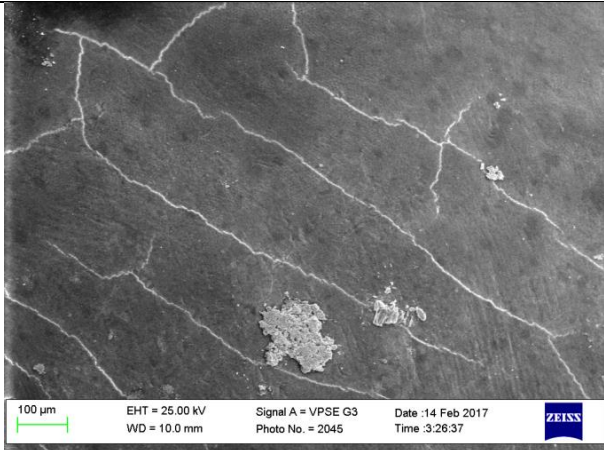
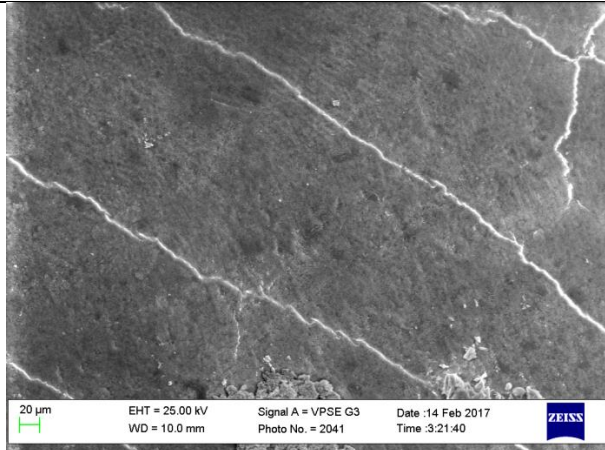
(38) Meyer-Lueckel H, Paris S. Infiltration of Natural Caries Lesions with Experimental Resins Differing in Penetration Coefficients and Ethanol Addition. *Caries Res.* 2010;44(4):408-414.

Appendix: SEM Images of Extracted Teeth

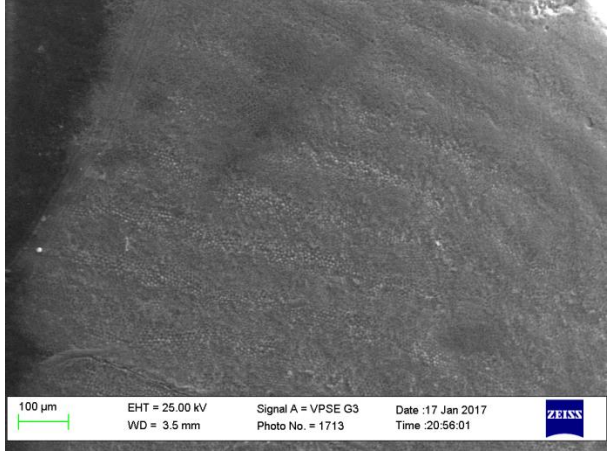
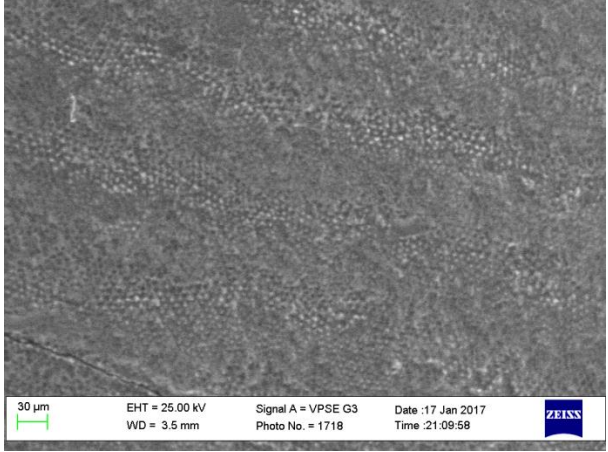
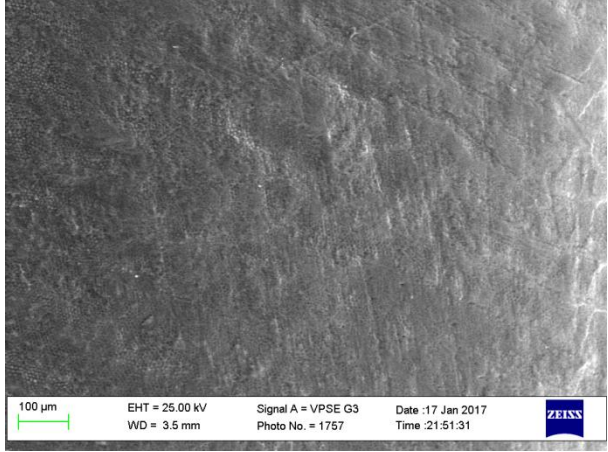
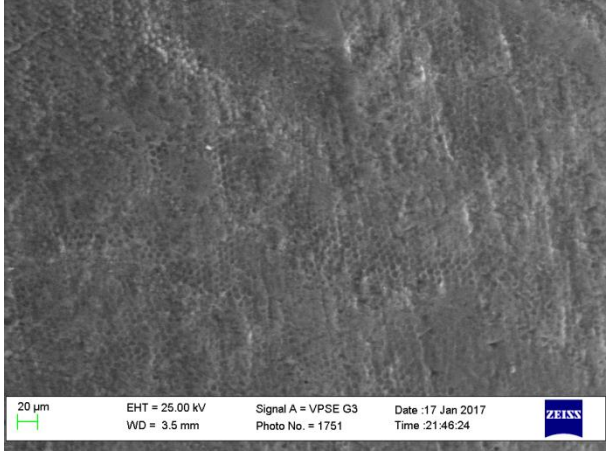
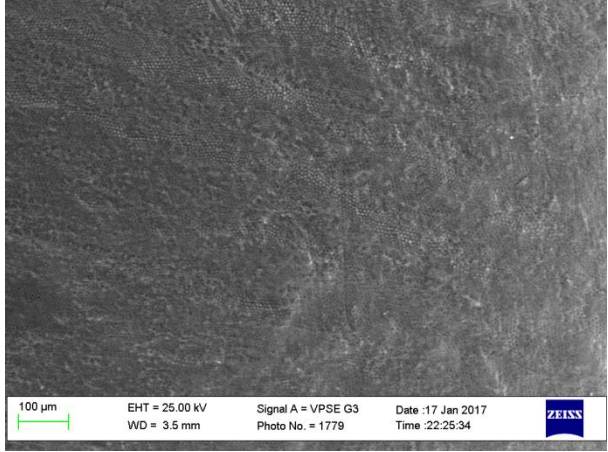
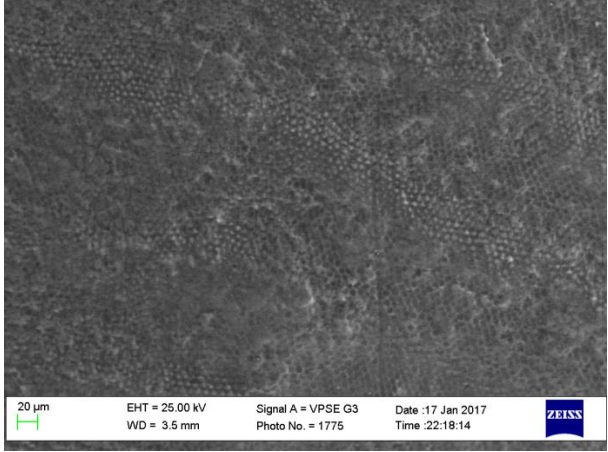
Tooth 1, T1

	250X	500X
Location A	 <p>100 µm EHT = 25.00 kV Signal A = VPSE G3 Date :17 Jan 2017 WD = 12.0 mm Photo No. = 1808 Time :23:10:02 ZEISS</p>	 <p>30 µm EHT = 25.00 kV Signal A = VPSE G3 Date :17 Jan 2017 WD = 12.0 mm Photo No. = 1801 Time :23:03:13 ZEISS</p>
Location B	 <p>100 µm EHT = 25.00 kV Signal A = VPSE G3 Date :17 Jan 2017 WD = 12.5 mm Photo No. = 1829 Time :23:31:00 ZEISS</p>	 <p>20 µm EHT = 25.00 kV Signal A = VPSE G3 Date :17 Jan 2017 WD = 12.5 mm Photo No. = 1823 Time :23:25:45 ZEISS</p>
Location C	 <p>100 µm EHT = 25.00 kV Signal A = VPSE G3 Date :17 Jan 2017 WD = 12.5 mm Photo No. = 1850 Time :23:47:36 ZEISS</p>	 <p>100 µm EHT = 25.00 kV Signal A = VPSE G3 Date :17 Jan 2017 WD = 12.5 mm Photo No. = 1850 Time :23:47:36 ZEISS</p>


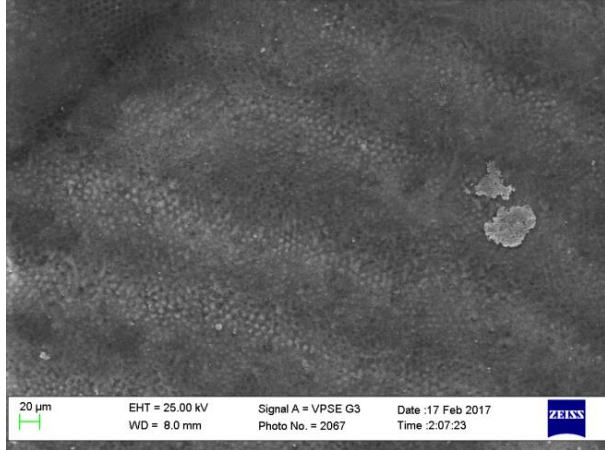

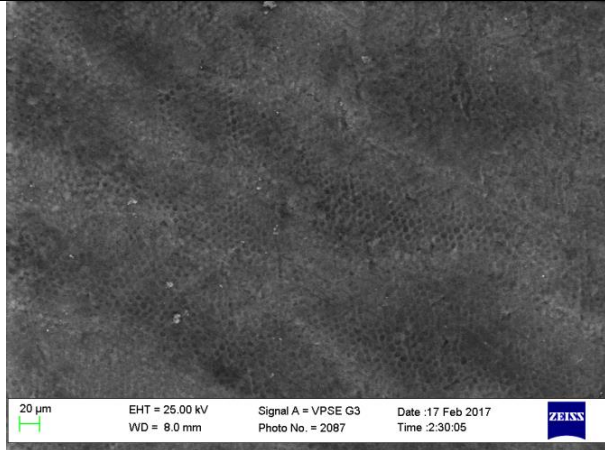

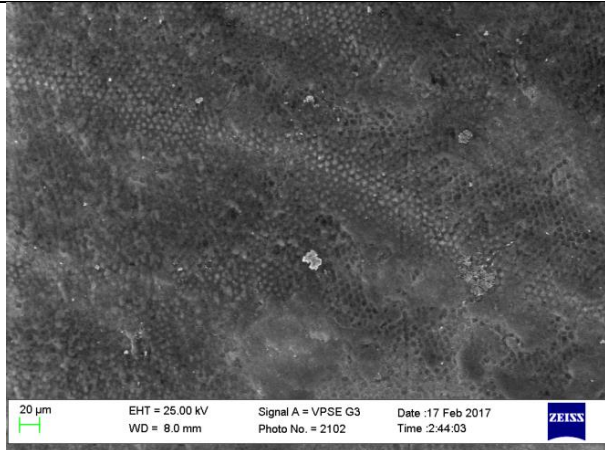
Tooth 1, T2

	250X	500X
Location A	 <p>100 µm EHT = 25.00 kV Signal A = VPSE G3 Date :14 Feb 2017 WD = 10.0 mm Photo No. = 2020 Time :2:43:27 ZEISS</p>	 <p>20 µm EHT = 25.00 kV Signal A = VPSE G3 Date :14 Feb 2017 WD = 10.0 mm Photo No. = 2013 Time :2:38:58 ZEISS</p>
Location B	 <p>100 µm EHT = 25.00 kV Signal A = VPSE G3 Date :14 Feb 2017 WD = 10.0 mm Photo No. = 2031 Time :2:56:15 ZEISS</p>	 <p>20 µm EHT = 25.00 kV Signal A = VPSE G3 Date :14 Feb 2017 WD = 10.0 mm Photo No. = 2025 Time :2:52:34 ZEISS</p>
Location C	 <p>100 µm EHT = 25.00 kV Signal A = VPSE G3 Date :14 Feb 2017 WD = 10.0 mm Photo No. = 2045 Time :3:26:37 ZEISS</p>	 <p>20 µm EHT = 25.00 kV Signal A = VPSE G3 Date :14 Feb 2017 WD = 10.0 mm Photo No. = 2041 Time :3:21:40 ZEISS</p>

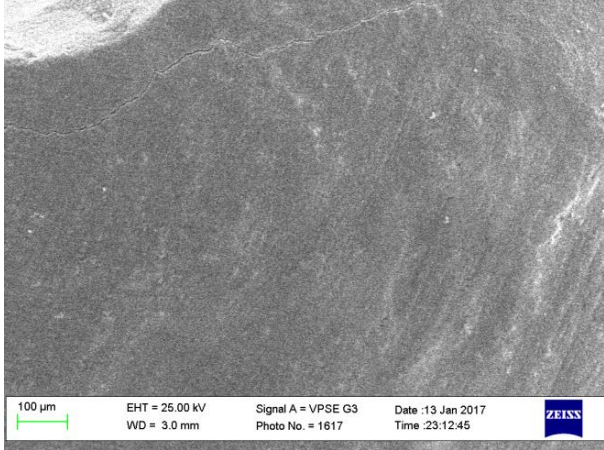
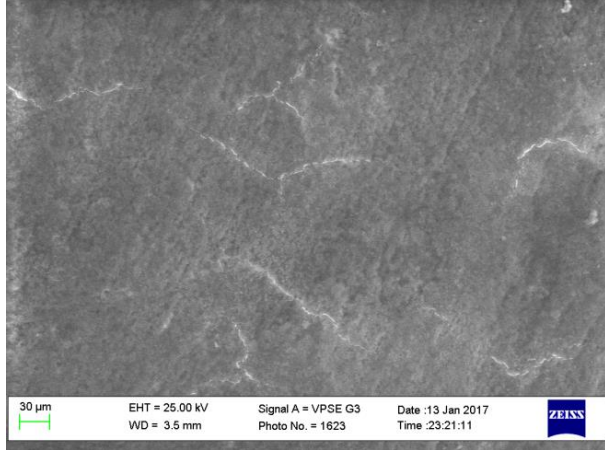
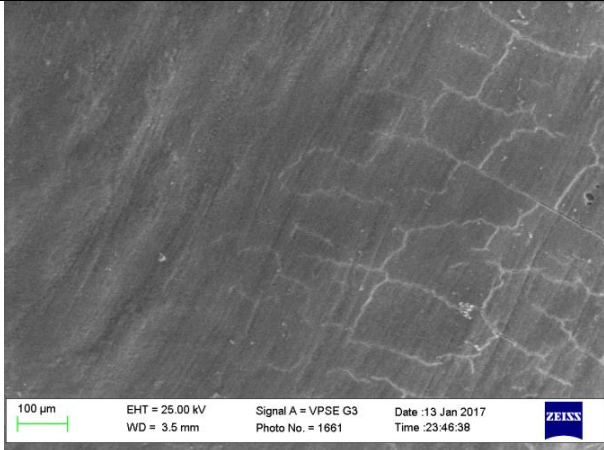
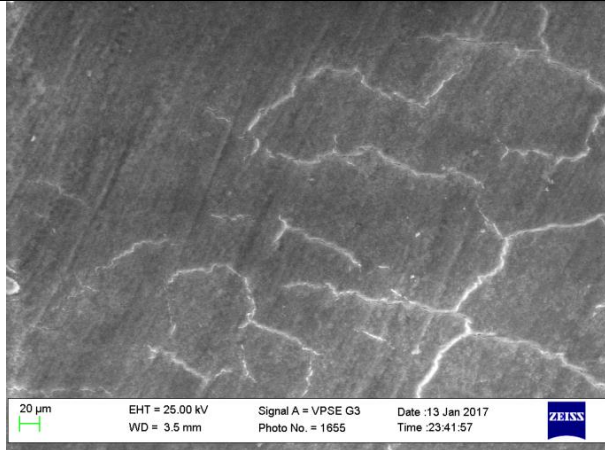
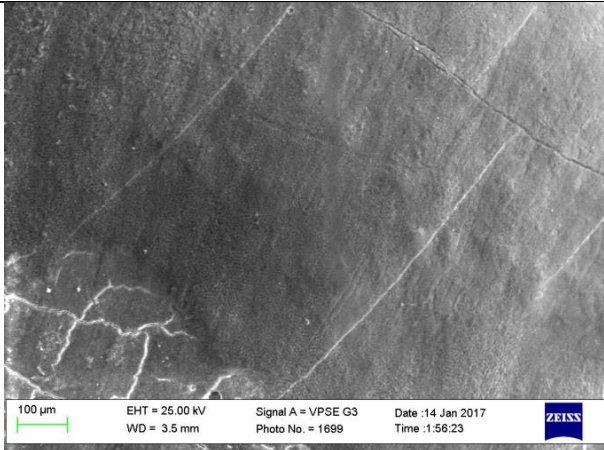

Tooth 2, T1

	250X	500X
Location A	 <p>100 μm EHT = 25.00 kV Signal A = VPSE G3 Date :17 Jan 2017 WD = 3.5 mm Photo No. = 1713 Time :20:56:01</p>	 <p>30 μm EHT = 25.00 kV Signal A = VPSE G3 Date :17 Jan 2017 WD = 3.5 mm Photo No. = 1718 Time :21:09:58</p>
Location B	 <p>100 μm EHT = 25.00 kV Signal A = VPSE G3 Date :17 Jan 2017 WD = 3.5 mm Photo No. = 1757 Time :21:51:31</p>	 <p>20 μm EHT = 25.00 kV Signal A = VPSE G3 Date :17 Jan 2017 WD = 3.5 mm Photo No. = 1751 Time :21:46:24</p>
Location C	 <p>100 μm EHT = 25.00 kV Signal A = VPSE G3 Date :17 Jan 2017 WD = 3.5 mm Photo No. = 1779 Time :22:25:34</p>	 <p>20 μm EHT = 25.00 kV Signal A = VPSE G3 Date :17 Jan 2017 WD = 3.5 mm Photo No. = 1775 Time :22:18:14</p>

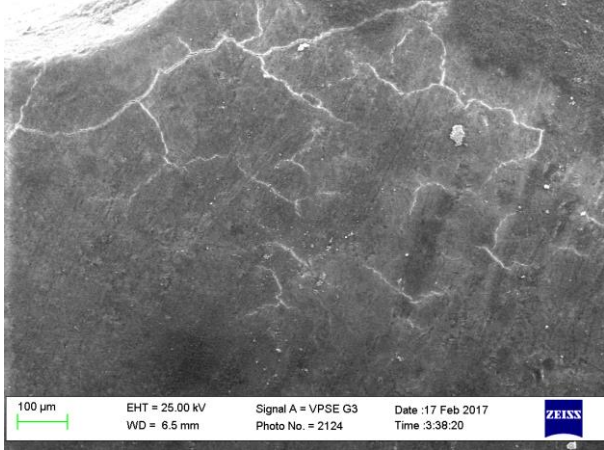
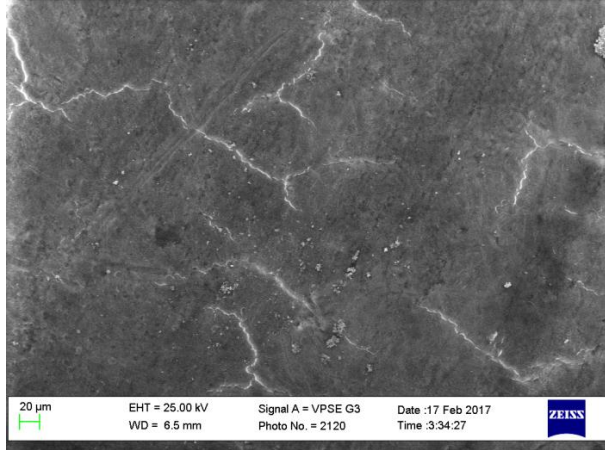
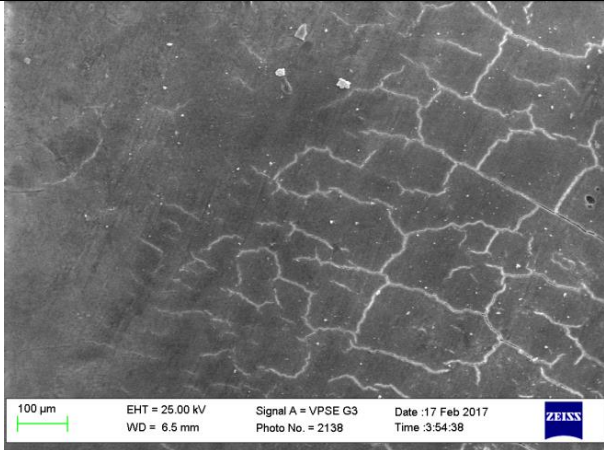
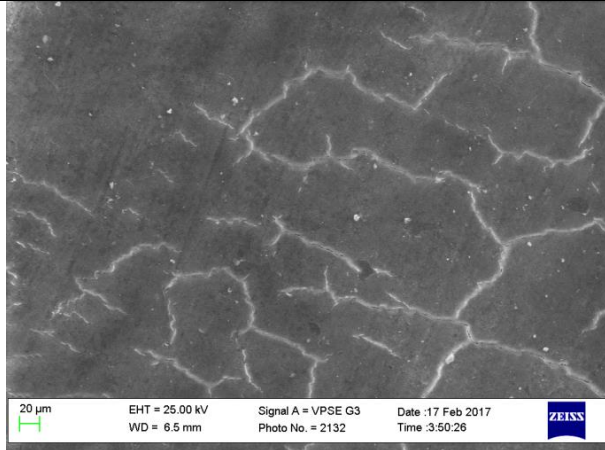


Tooth 2, T2

	250X	500X
Location A	 <p>100 µm EHT = 25.00 kV Signal A = VPSE G3 Date :17 Feb 2017 WD = 8.0 mm Photo No. = 2075 Time :2:14:15 ZEISS</p>	 <p>20 µm EHT = 25.00 kV Signal A = VPSE G3 Date :17 Feb 2017 WD = 8.0 mm Photo No. = 2067 Time :2:07:23 ZEISS</p>
Location B	 <p>100 µm EHT = 25.00 kV Signal A = VPSE G3 Date :17 Feb 2017 WD = 8.0 mm Photo No. = 2095 Time :2:35:55 ZEISS</p>	 <p>20 µm EHT = 25.00 kV Signal A = VPSE G3 Date :17 Feb 2017 WD = 8.0 mm Photo No. = 2087 Time :2:30:05 ZEISS</p>
Location C	 <p>100 µm EHT = 25.00 kV Signal A = VPSE G3 Date :17 Feb 2017 WD = 8.0 mm Photo No. = 2106 Time :2:52:52 ZEISS</p>	 <p>20 µm EHT = 25.00 kV Signal A = VPSE G3 Date :17 Feb 2017 WD = 8.0 mm Photo No. = 2102 Time :2:44:03 ZEISS</p>

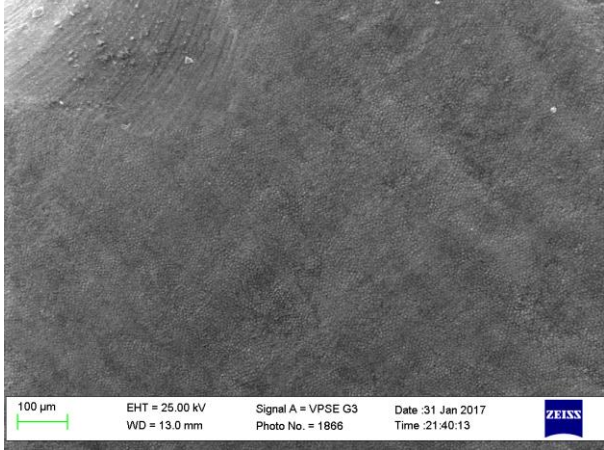
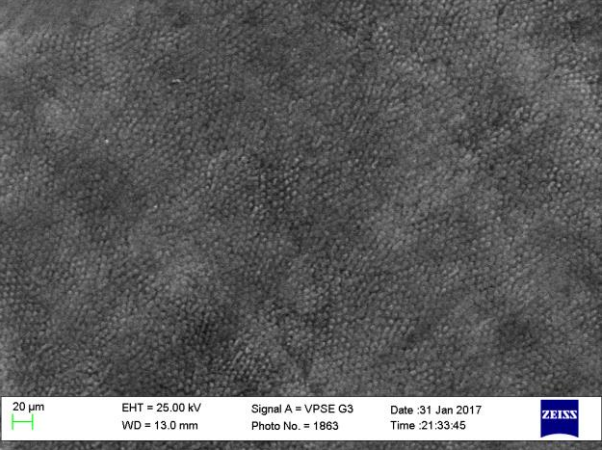
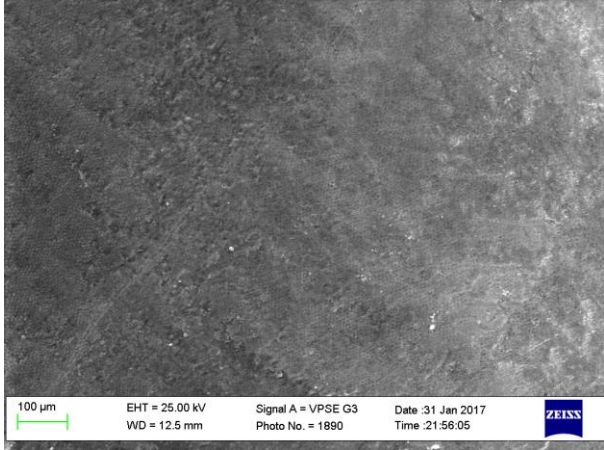
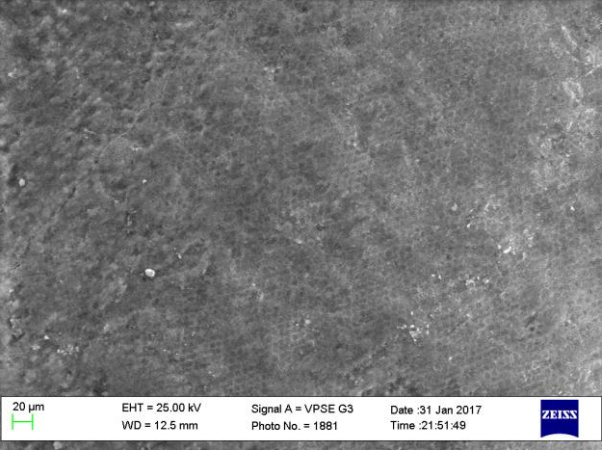
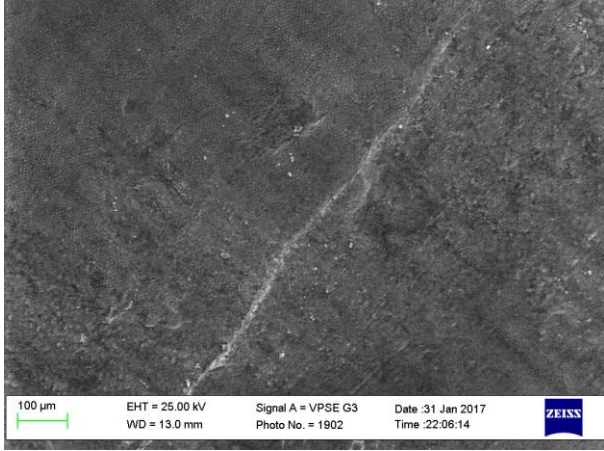
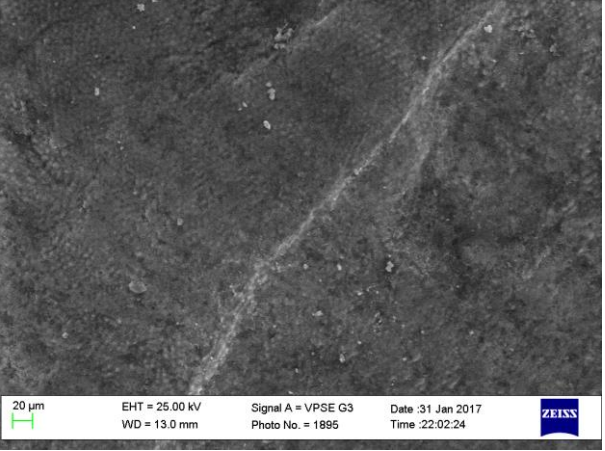
Tooth 3, T1

	250X	500X
Location A	 <p>100 µm EHT = 25.00 kV Signal A = VPSE G3 Date :13 Jan 2017 WD = 3.0 mm Photo No. = 1617 Time :23:12:45 ZEISS</p>	 <p>30 µm EHT = 25.00 kV Signal A = VPSE G3 Date :13 Jan 2017 WD = 3.5 mm Photo No. = 1623 Time :23:21:11 ZEISS</p>
Location B	 <p>100 µm EHT = 25.00 kV Signal A = VPSE G3 Date :13 Jan 2017 WD = 3.5 mm Photo No. = 1661 Time :23:46:38 ZEISS</p>	 <p>20 µm EHT = 25.00 kV Signal A = VPSE G3 Date :13 Jan 2017 WD = 3.5 mm Photo No. = 1655 Time :23:41:57 ZEISS</p>
Location C	 <p>100 µm EHT = 25.00 kV Signal A = VPSE G3 Date :14 Jan 2017 WD = 3.5 mm Photo No. = 1699 Time :1:56:23 ZEISS</p>	 <p>20 µm EHT = 25.00 kV Signal A = VPSE G3 Date :14 Jan 2017 WD = 3.5 mm Photo No. = 1692 Time :1:41:47 ZEISS</p>


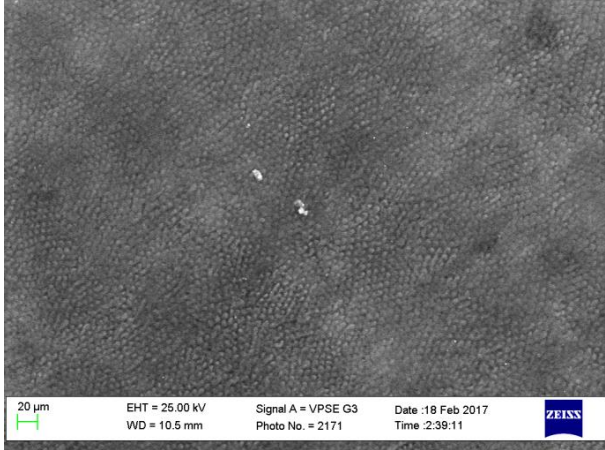

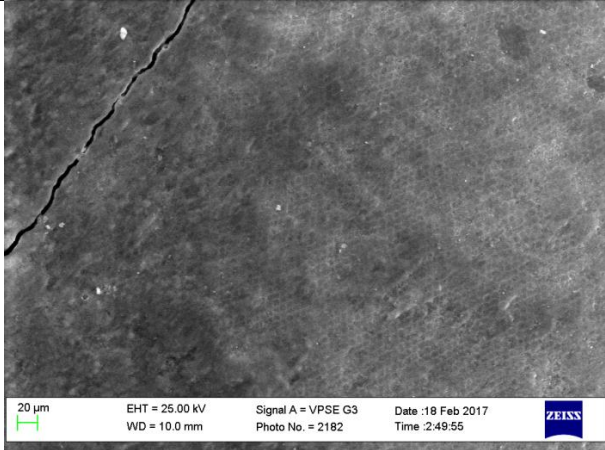

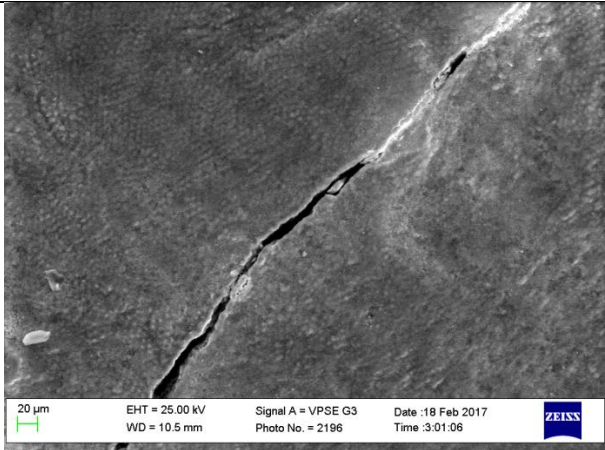
Tooth 3, T2

	250X	500X
Location A	 <p>100 µm EHT = 25.00 kV Signal A = VPSE G3 Date :17 Feb 2017 WD = 6.5 mm Photo No. = 2124 Time :3:38:20 ZEISS</p>	 <p>20 µm EHT = 25.00 kV Signal A = VPSE G3 Date :17 Feb 2017 WD = 6.5 mm Photo No. = 2120 Time :3:34:27 ZEISS</p>
Location B	 <p>100 µm EHT = 25.00 kV Signal A = VPSE G3 Date :17 Feb 2017 WD = 6.5 mm Photo No. = 2138 Time :3:54:38 ZEISS</p>	 <p>20 µm EHT = 25.00 kV Signal A = VPSE G3 Date :17 Feb 2017 WD = 6.5 mm Photo No. = 2132 Time :3:50:26 ZEISS</p>
Location C	 <p>100 µm EHT = 25.00 kV Signal A = VPSE G3 Date :18 Feb 2017 WD = 7.5 mm Photo No. = 2153 Time :1:25:02 ZEISS</p>	 <p>20 µm EHT = 25.00 kV Signal A = VPSE G3 Date :18 Feb 2017 WD = 7.5 mm Photo No. = 2148 Time :1:19:08 ZEISS</p>

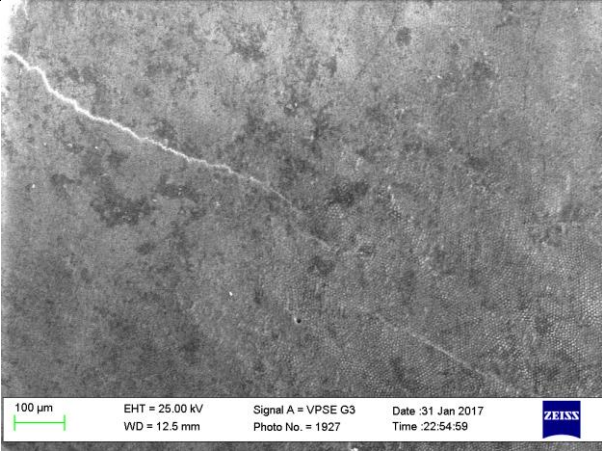
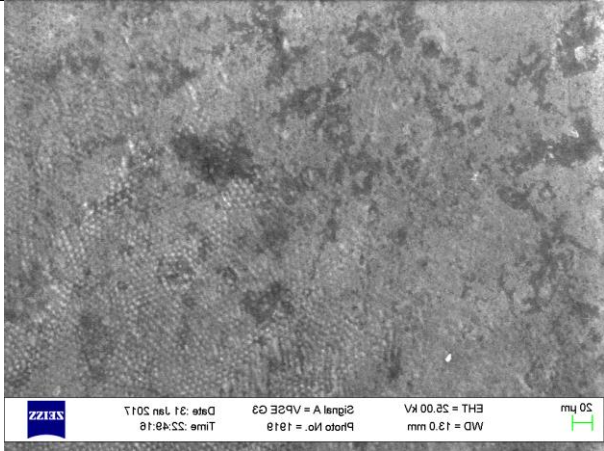
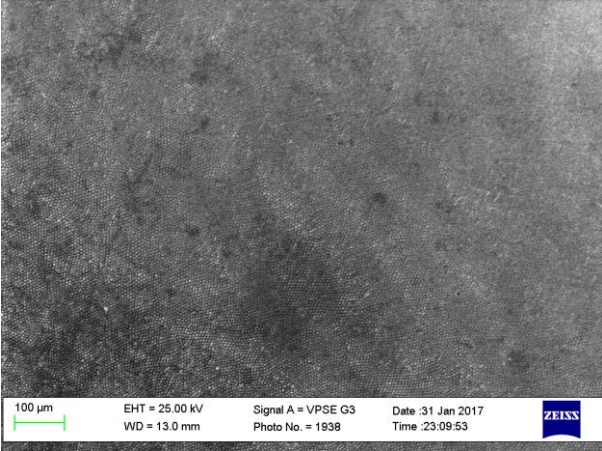
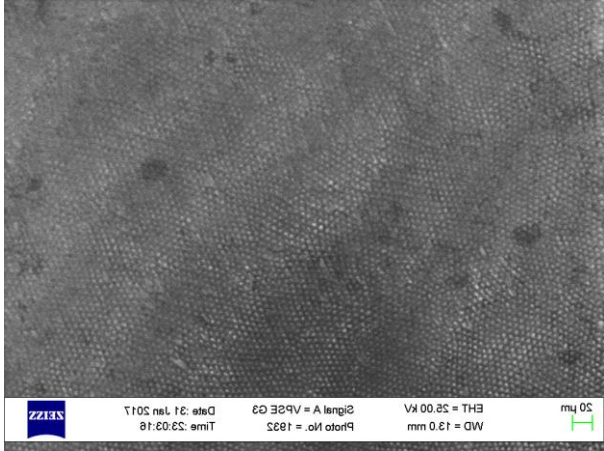
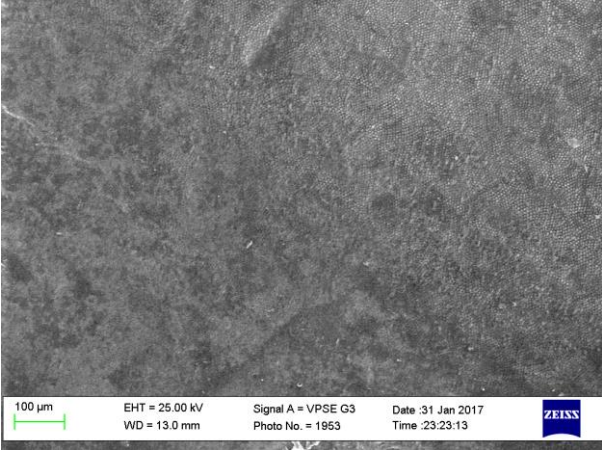
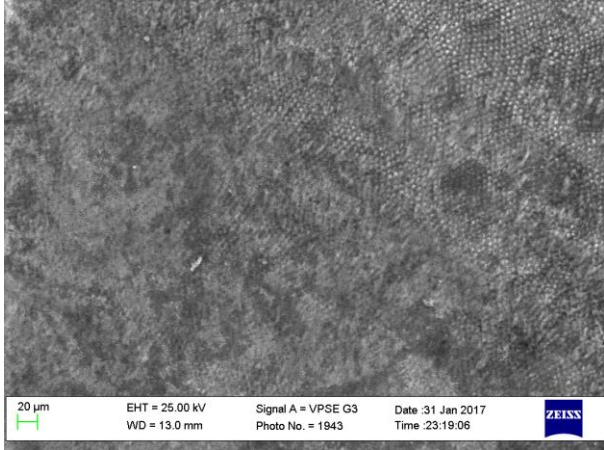
Tooth 4, T1

	250X	500X
Location A		
Location B		
Location C		

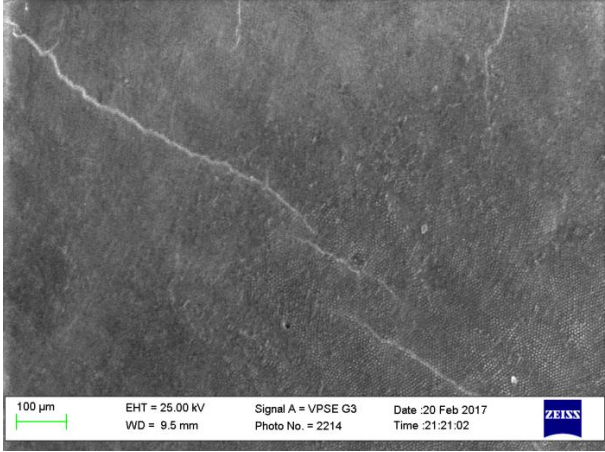
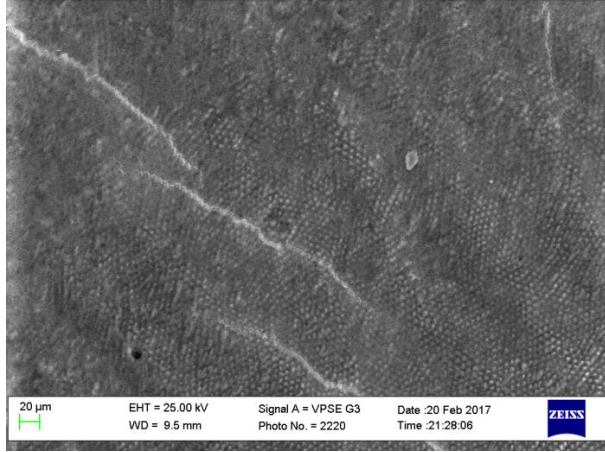

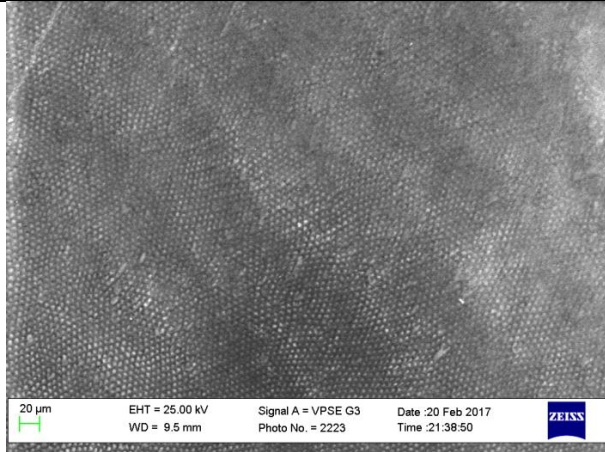
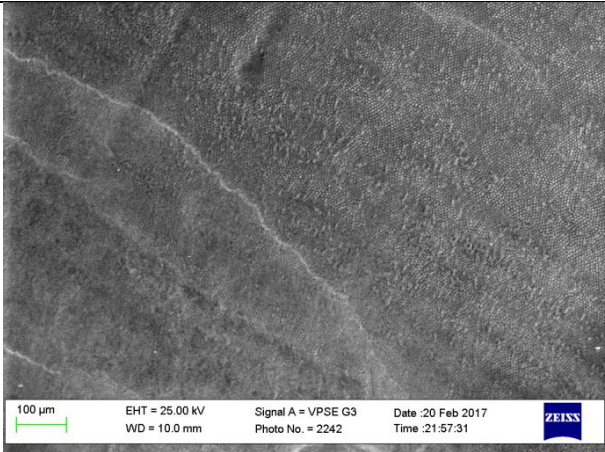
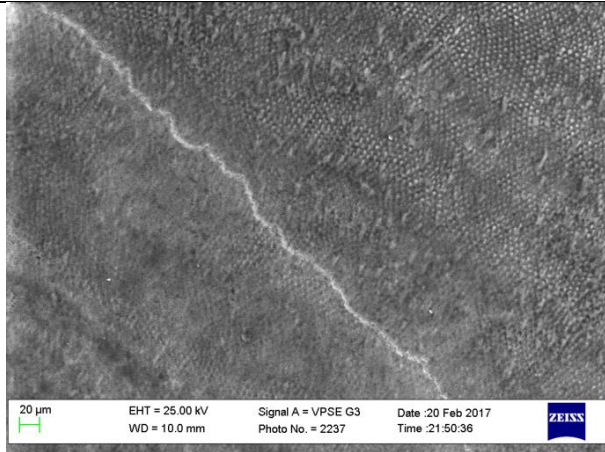
Tooth 4, T2

	250X	500X
Location A		
Location B		
Location C		

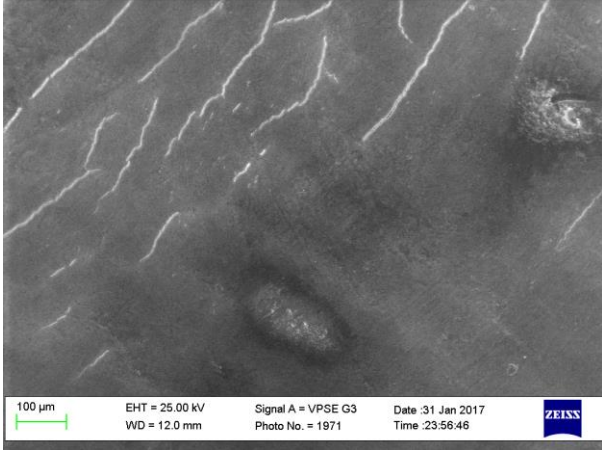
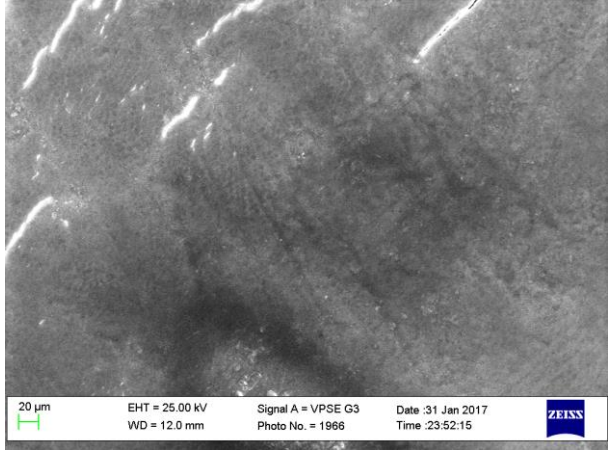
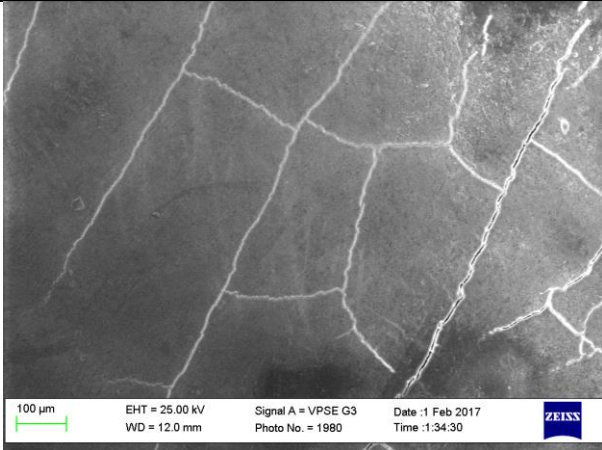
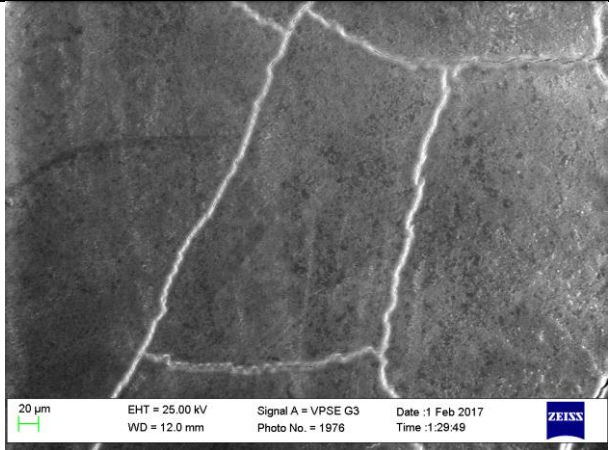

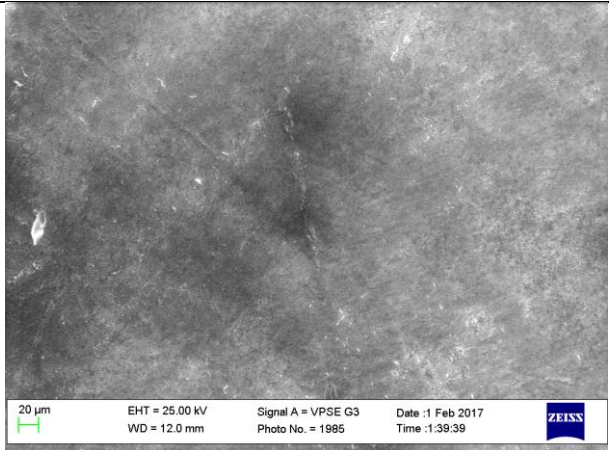
Tooth 5, T1

	250X	500X
Location A	 <p>100 µm EHT = 25.00 kV Signal A = VPSE G3 Date :31 Jan 2017 WD = 12.5 mm Photo No. = 1927 Time :22:54:59 ZEISS</p>	 <p>ZEISS EHT = 25.00 kV Signal A = VPSE G3 Date :31 Jan 2017 WD 12.0 mm Photo No. = 1918 Time :23:49:18</p>
Location B	 <p>100 µm EHT = 25.00 kV Signal A = VPSE G3 Date :31 Jan 2017 WD = 13.0 mm Photo No. = 1938 Time :23:09:53 ZEISS</p>	 <p>ZEISS EHT = 25.00 kV Signal A = VPSE G3 Date :31 Jan 2017 WD 13.0 mm Photo No. = 1935 Time :23:03:18</p>
Location C	 <p>100 µm EHT = 25.00 kV Signal A = VPSE G3 Date :31 Jan 2017 WD = 13.0 mm Photo No. = 1953 Time :23:23:13 ZEISS</p>	 <p>20 µm EHT = 25.00 kV Signal A = VPSE G3 Date :31 Jan 2017 WD = 13.0 mm Photo No. = 1943 Time :23:19:06 ZEISS</p>

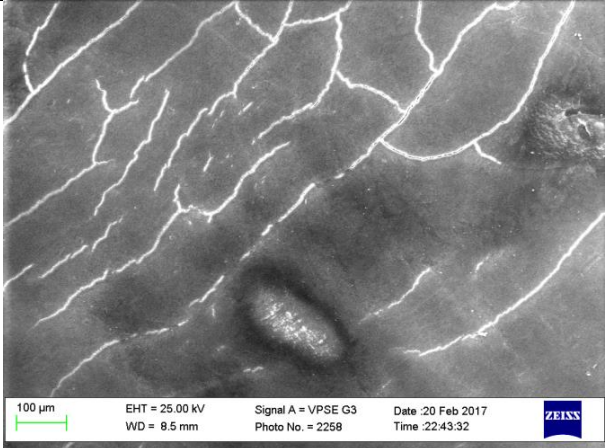
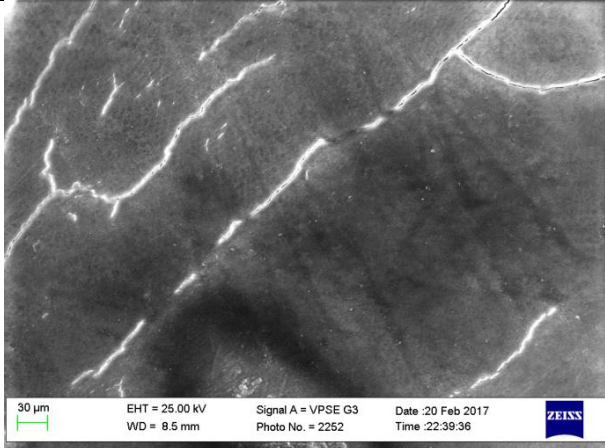
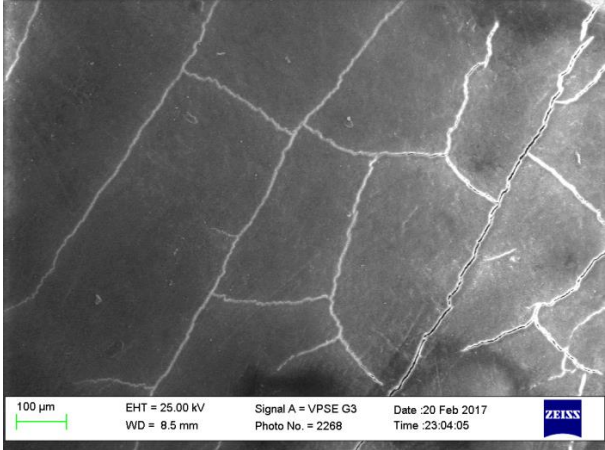
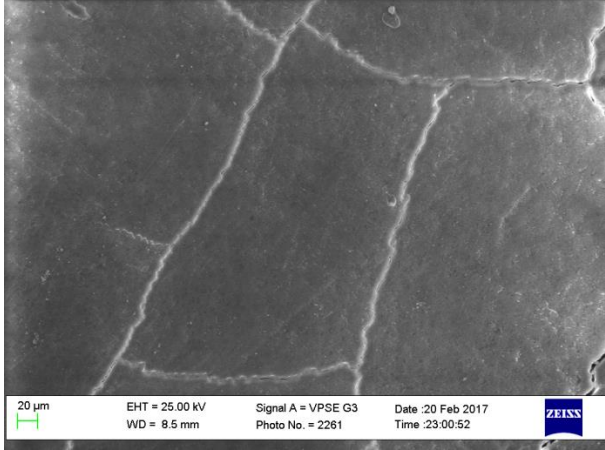
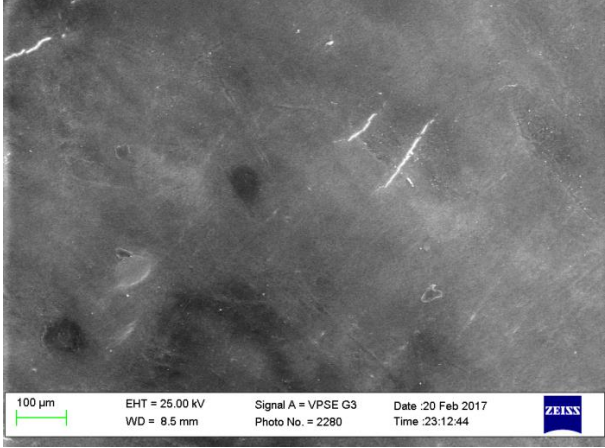
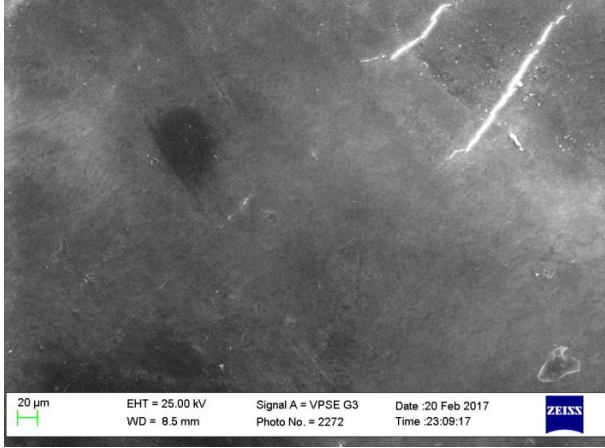
Tooth 5, T2

	250X	500X
Location A		
Location B		
Location C		

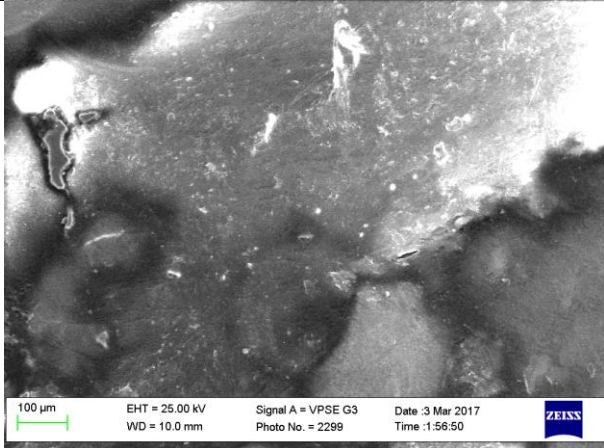
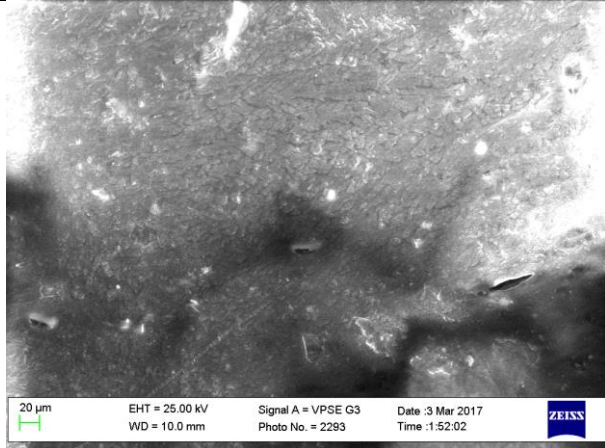

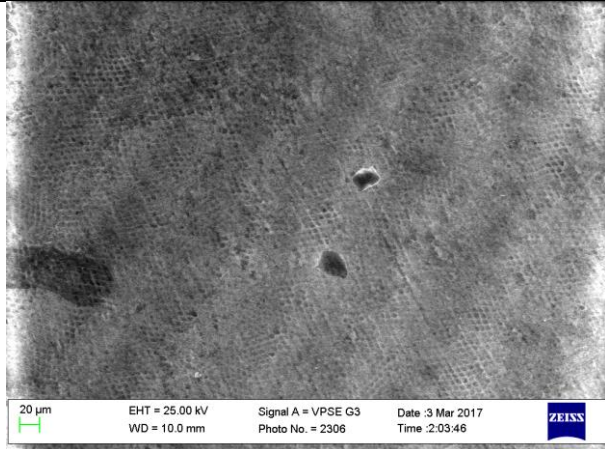
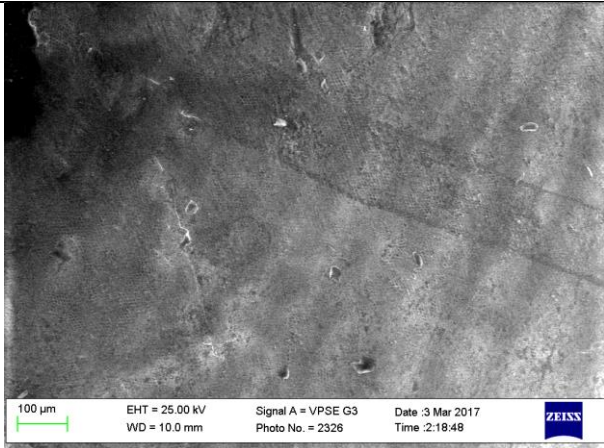

Tooth 6, T1

	250X	500X
Location A	 <p>100 μm EHT = 25.00 kV Signal A = VPSE G3 Date :31 Jan 2017 WD = 12.0 mm Photo No. = 1971 Time :23:56:46 ZEISS</p>	 <p>20 μm EHT = 25.00 kV Signal A = VPSE G3 Date :31 Jan 2017 WD = 12.0 mm Photo No. = 1966 Time :23:52:15 ZEISS</p>
Location B	 <p>100 μm EHT = 25.00 kV Signal A = VPSE G3 Date :1 Feb 2017 WD = 12.0 mm Photo No. = 1980 Time :1:34:30 ZEISS</p>	 <p>20 μm EHT = 25.00 kV Signal A = VPSE G3 Date :1 Feb 2017 WD = 12.0 mm Photo No. = 1976 Time :1:29:49 ZEISS</p>
Location C	 <p>100 μm EHT = 25.00 kV Signal A = VPSE G3 Date :1 Feb 2017 WD = 12.0 mm Photo No. = 2003 Time :2:02:47 ZEISS</p>	 <p>20 μm EHT = 25.00 kV Signal A = VPSE G3 Date :1 Feb 2017 WD = 12.0 mm Photo No. = 1985 Time :1:39:39 ZEISS</p>

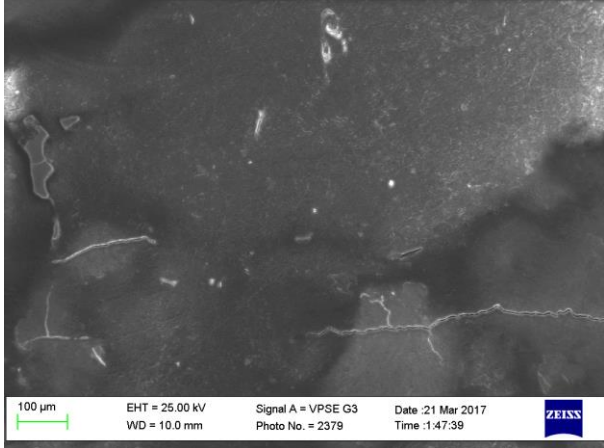
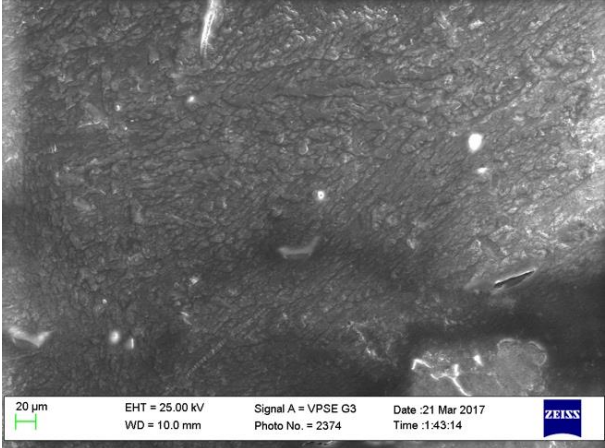
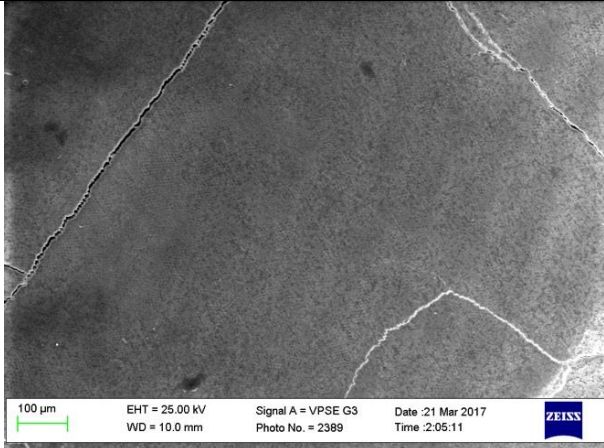
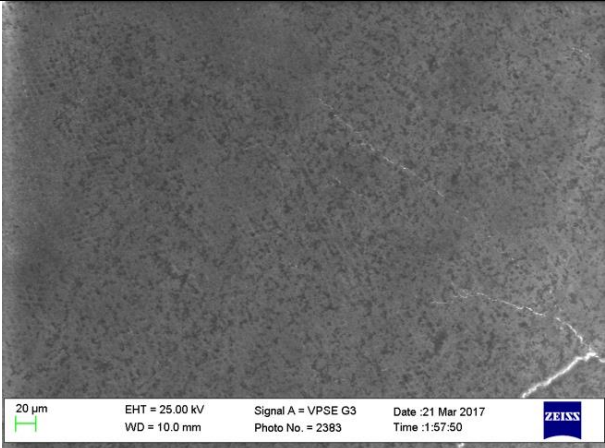
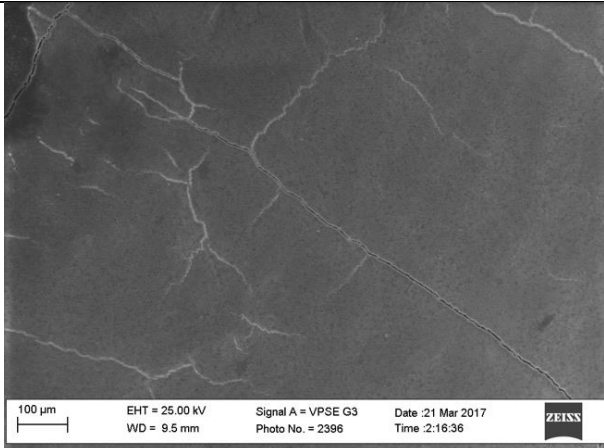
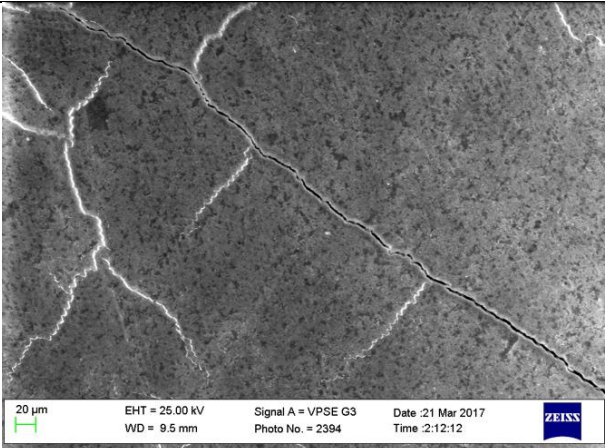
Tooth 6, T2

	250X	500X
Location A		
Location B		
Location C		

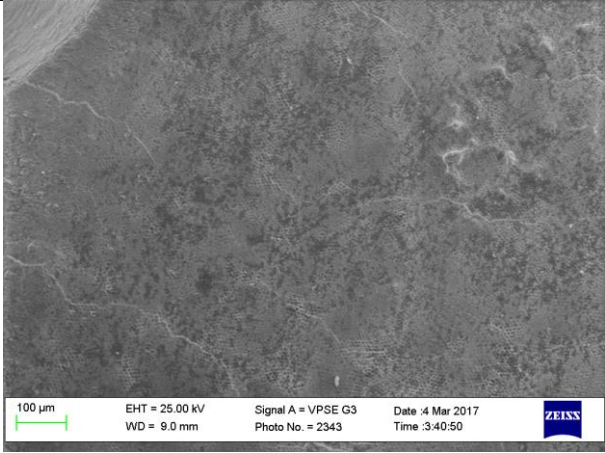
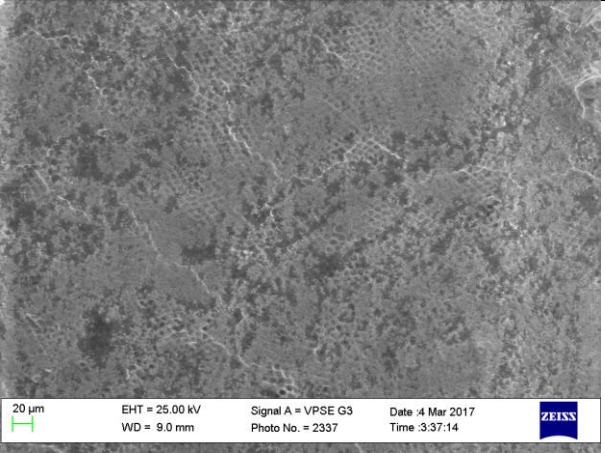
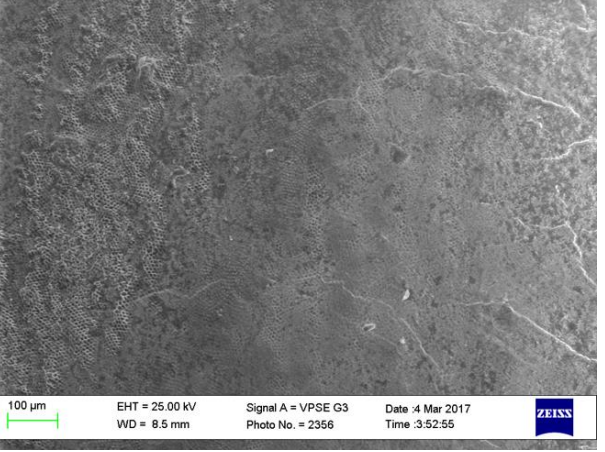
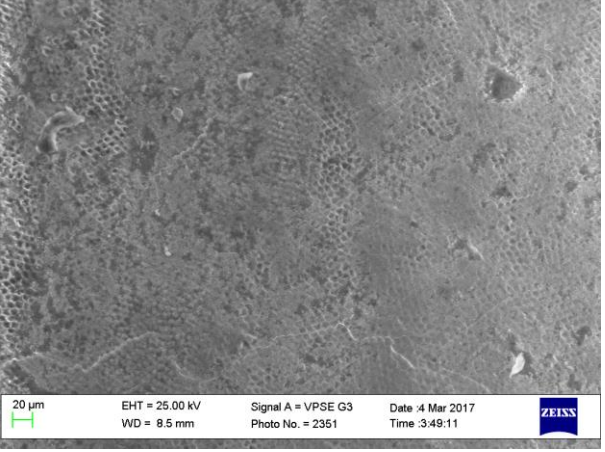
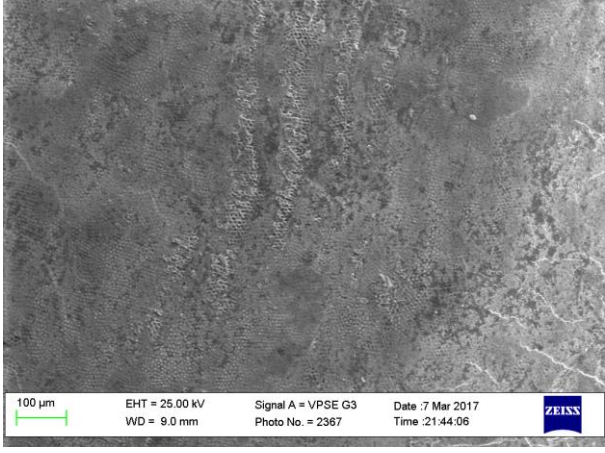
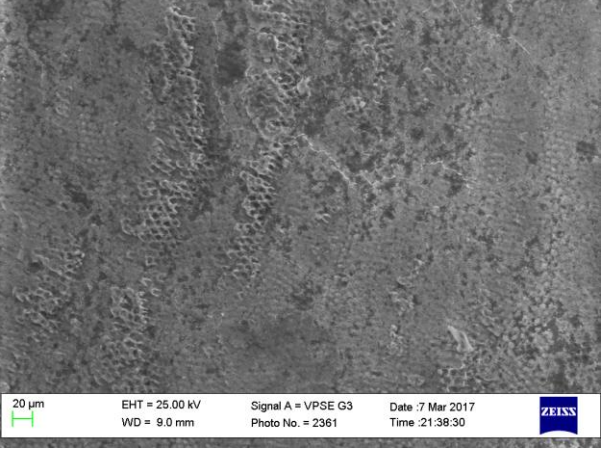
Tooth 7, T1

	250X	500X
Location A	 <p>100 μm EHT = 25.00 kV Signal A = VPSE G3 Date :3 Mar 2017 WD = 10.0 mm Photo No. = 2299 Time :1:56:50 ZEISS</p>	 <p>20 μm EHT = 25.00 kV Signal A = VPSE G3 Date :3 Mar 2017 WD = 10.0 mm Photo No. = 2293 Time :1:52:02 ZEISS</p>
Location B	 <p>100 μm EHT = 25.00 kV Signal A = VPSE G3 Date :3 Mar 2017 WD = 10.0 mm Photo No. = 2311 Time :2:08:31 ZEISS</p>	 <p>20 μm EHT = 25.00 kV Signal A = VPSE G3 Date :3 Mar 2017 WD = 10.0 mm Photo No. = 2306 Time :2:03:46 ZEISS</p>
Location C	 <p>100 μm EHT = 25.00 kV Signal A = VPSE G3 Date :3 Mar 2017 WD = 10.0 mm Photo No. = 2326 Time :2:18:48 ZEISS</p>	 <p>20 μm EHT = 25.00 kV Signal A = VPSE G3 Date :3 Mar 2017 WD = 10.0 mm Photo No. = 2319 Time :2:15:00 ZEISS</p>


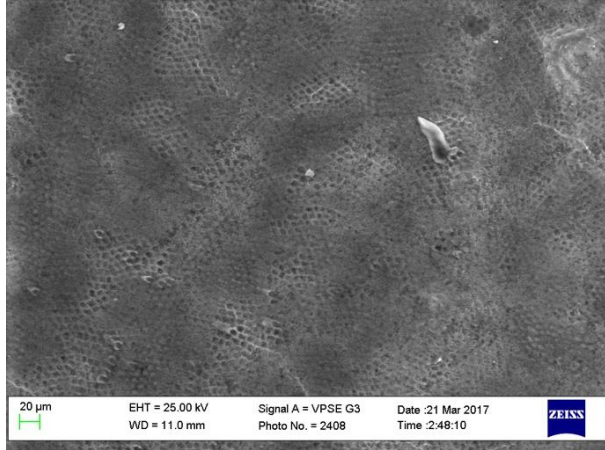

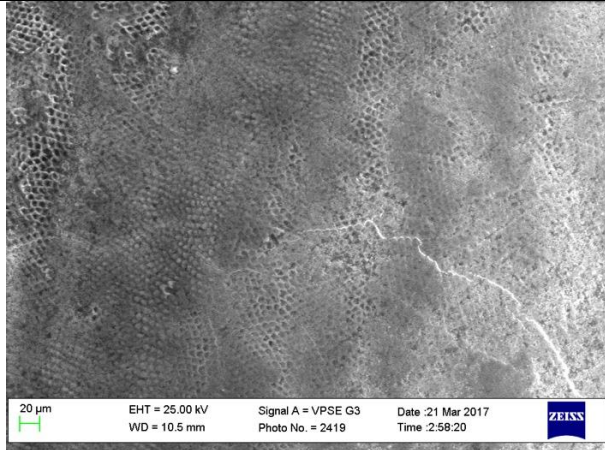
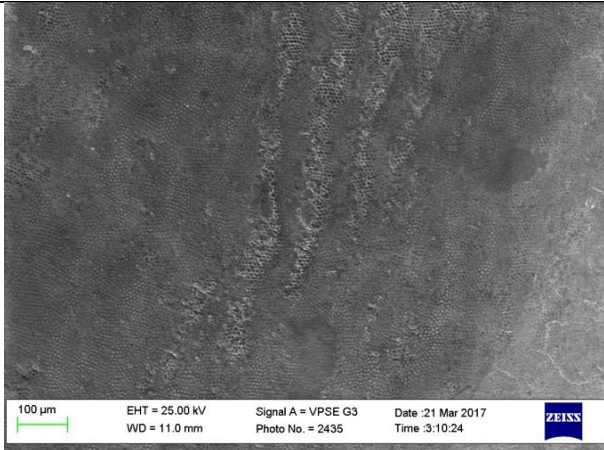
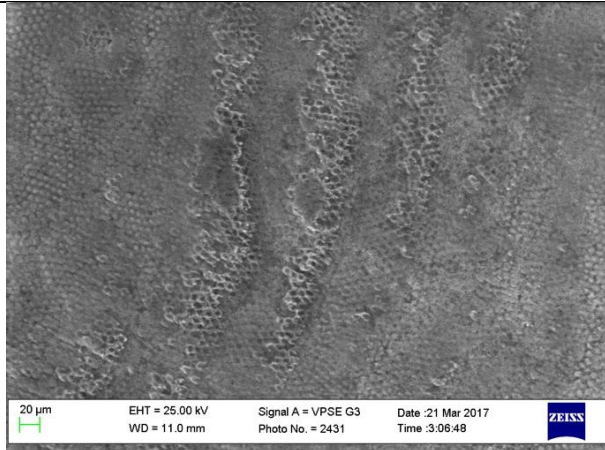
Tooth 7, T2

	250X	500X
Location A	 <p>100 μm EHT = 25.00 kV Signal A = VPSE G3 Date :21 Mar 2017 WD = 10.0 mm Photo No. = 2379 Time :1:47:39 ZEISS</p>	 <p>20 μm EHT = 25.00 kV Signal A = VPSE G3 Date :21 Mar 2017 WD = 10.0 mm Photo No. = 2374 Time :1:43:14 ZEISS</p>
Location B	 <p>100 μm EHT = 25.00 kV Signal A = VPSE G3 Date :21 Mar 2017 WD = 10.0 mm Photo No. = 2389 Time :2:05:11 ZEISS</p>	 <p>20 μm EHT = 25.00 kV Signal A = VPSE G3 Date :21 Mar 2017 WD = 10.0 mm Photo No. = 2383 Time :1:57:50 ZEISS</p>
Location C	 <p>100 μm EHT = 25.00 kV Signal A = VPSE G3 Date :21 Mar 2017 WD = 9.5 mm Photo No. = 2396 Time :2:16:36 ZEISS</p>	 <p>20 μm EHT = 25.00 kV Signal A = VPSE G3 Date :21 Mar 2017 WD = 9.5 mm Photo No. = 2394 Time :2:12:12 ZEISS</p>


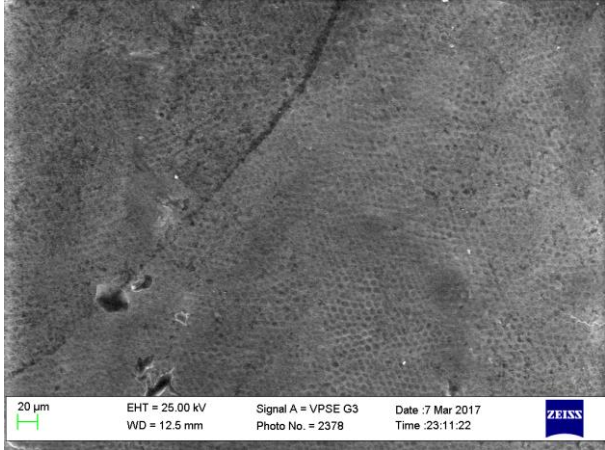




Tooth 8, T1

	250X	500X
Location A		
Location B		
Location C		

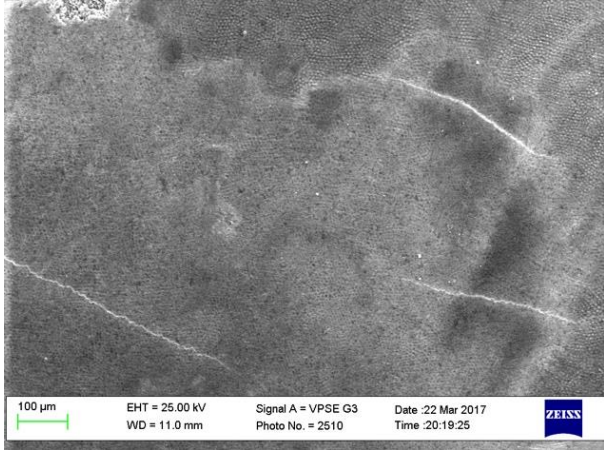
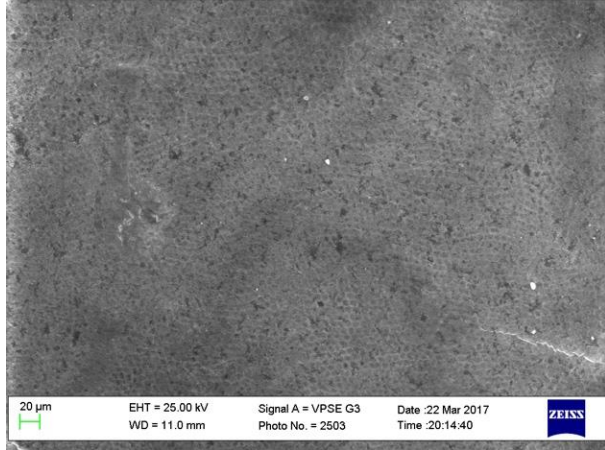
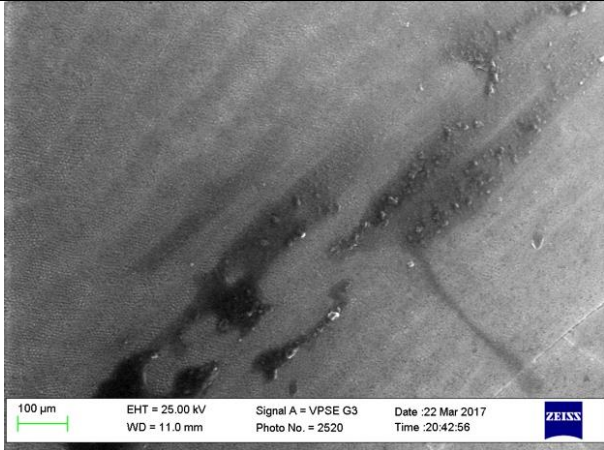
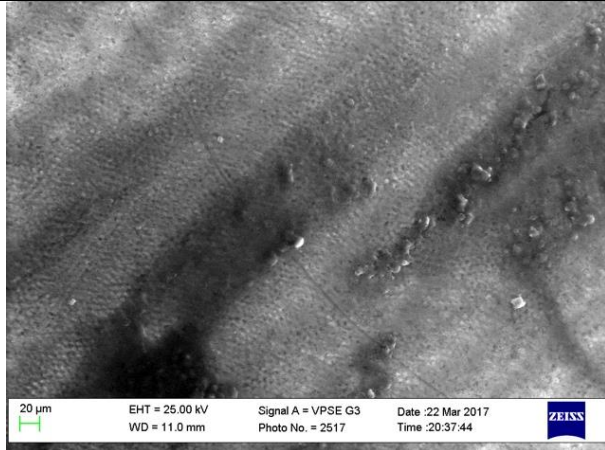


Tooth 8, T2

	250X	500X
Location A	 <p>100 µm EHT = 25.00 kV Signal A = VPSE G3 Date :21 Mar 2017 WD = 11.0 mm Photo No. = 2414 Time :2:53:31 ZEISS</p>	 <p>20 µm EHT = 25.00 kV Signal A = VPSE G3 Date :21 Mar 2017 WD = 11.0 mm Photo No. = 2498 Time :2:48:10 ZEISS</p>
Location B	 <p>100 µm EHT = 25.00 kV Signal A = VPSE G3 Date :21 Mar 2017 WD = 10.5 mm Photo No. = 2425 Time :3:01:42 ZEISS</p>	 <p>20 µm EHT = 25.00 kV Signal A = VPSE G3 Date :21 Mar 2017 WD = 10.5 mm Photo No. = 2419 Time :2:58:20 ZEISS</p>
Location C	 <p>100 µm EHT = 25.00 kV Signal A = VPSE G3 Date :21 Mar 2017 WD = 11.0 mm Photo No. = 2435 Time :3:10:24 ZEISS</p>	 <p>20 µm EHT = 25.00 kV Signal A = VPSE G3 Date :21 Mar 2017 WD = 11.0 mm Photo No. = 2431 Time :3:06:48 ZEISS</p>

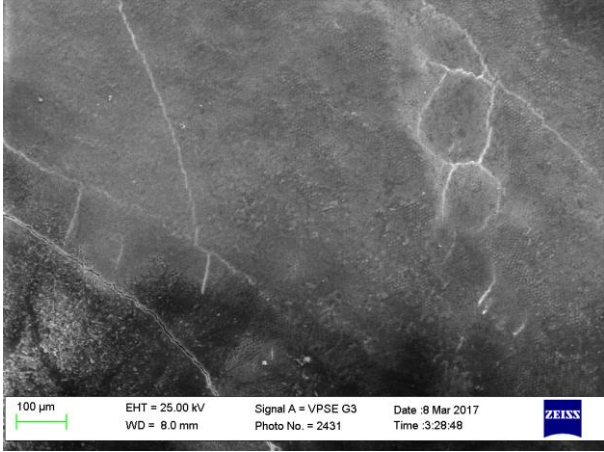


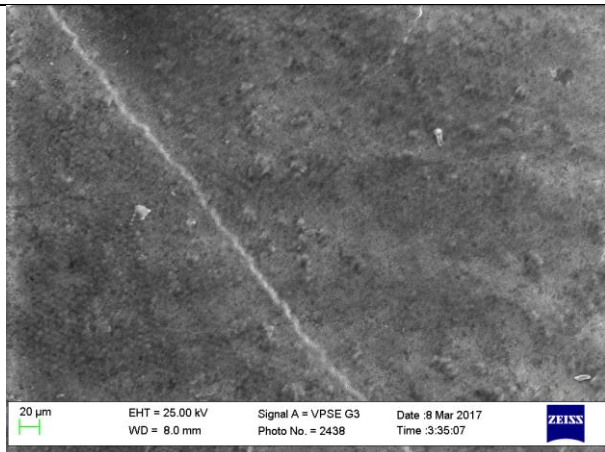

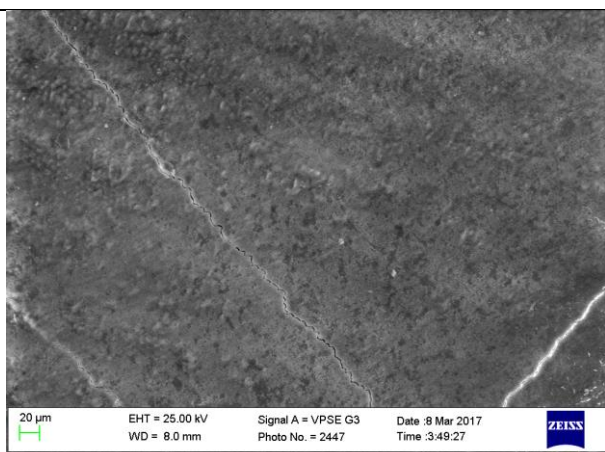
Tooth 9, T1

	250X	500X
Location A	 <p>100 μm EHT = 25.00 kV Signal A = VPSE G3 Date :7 Mar 2017 WD = 12.5 mm Photo No. = 2383 Time :23:21:06 ZEISS</p>	 <p>20 μm EHT = 25.00 kV Signal A = VPSE G3 Date :7 Mar 2017 WD = 12.5 mm Photo No. = 2378 Time :23:11:22 ZEISS</p>
Location B	 <p>100 μm EHT = 25.00 kV Signal A = VPSE G3 Date :7 Mar 2017 WD = 12.5 mm Photo No. = 2384 Time :23:42:22 ZEISS</p>	 <p>20 μm EHT = 25.00 kV Signal A = VPSE G3 Date :7 Mar 2017 WD = 13.0 mm Photo No. = 2390 Time :23:31:53 ZEISS</p>
Location C	 <p>100 μm EHT = 25.00 kV Signal A = VPSE G3 Date :8 Mar 2017 WD = 12.5 mm Photo No. = 2408 Time :0:19:35 ZEISS</p>	 <p>20 μm EHT = 25.00 kV Signal A = VPSE G3 Date :8 Mar 2017 WD = 12.5 mm Photo No. = 2401 Time :0:15:55 ZEISS</p>

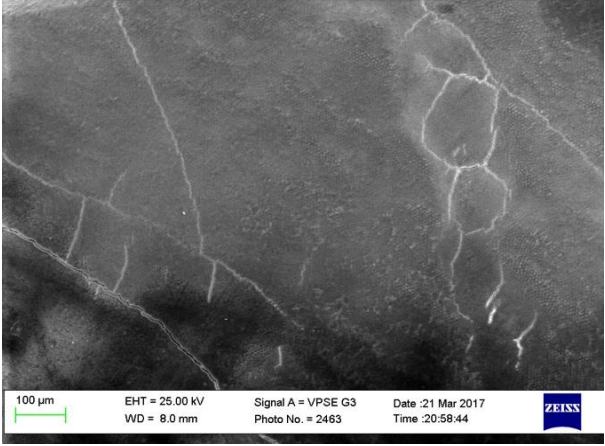
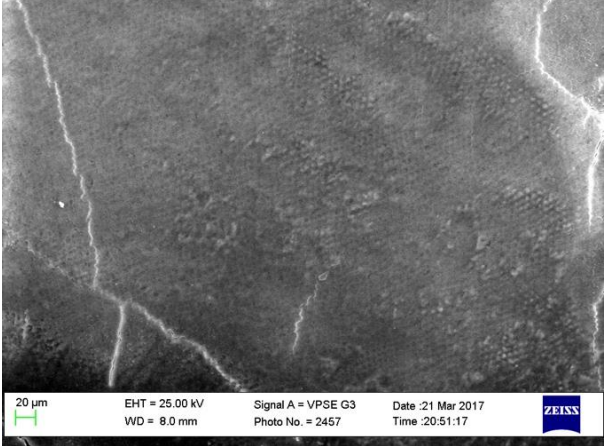

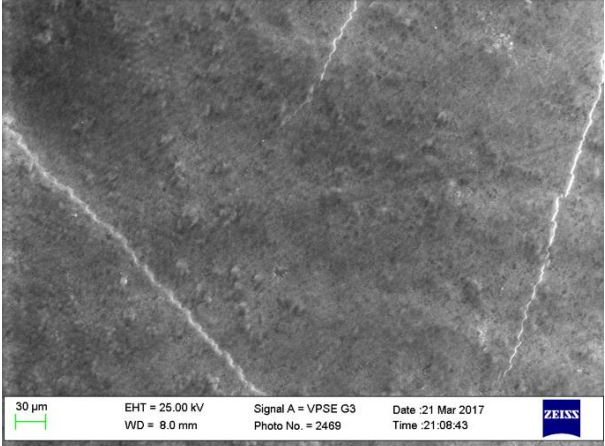

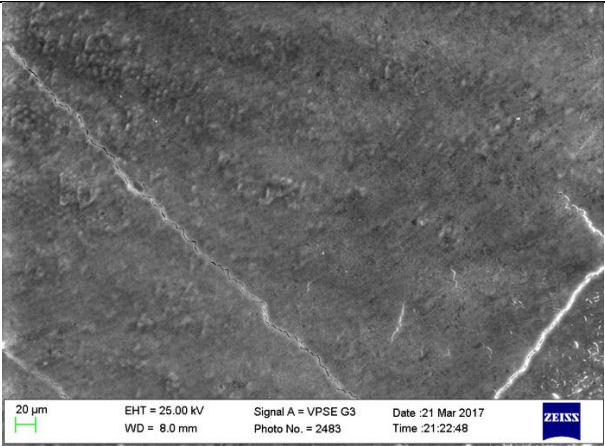
Tooth 9, T2

	250X	500X
Location A	 <p>100 µm EHT = 25.00 kV Signal A = VPSE G3 Date :22 Mar 2017 WD = 11.0 mm Photo No. = 2510 Time :20:19:25 ZEISS</p>	 <p>20 µm EHT = 25.00 kV Signal A = VPSE G3 Date :22 Mar 2017 WD = 11.0 mm Photo No. = 2503 Time :20:14:40 ZEISS</p>
Location B	 <p>100 µm EHT = 25.00 kV Signal A = VPSE G3 Date :22 Mar 2017 WD = 11.0 mm Photo No. = 2520 Time :20:42:56 ZEISS</p>	 <p>20 µm EHT = 25.00 kV Signal A = VPSE G3 Date :22 Mar 2017 WD = 11.0 mm Photo No. = 2517 Time :20:37:44 ZEISS</p>
Location C	 <p>100 µm EHT = 25.00 kV Signal A = VPSE G3 Date :22 Mar 2017 WD = 11.5 mm Photo No. = 2534 Time :20:54:23 ZEISS</p>	 <p>20 µm EHT = 25.00 kV Signal A = VPSE G3 Date :22 Mar 2017 WD = 11.5 mm Photo No. = 2530 Time :20:50:20 ZEISS</p>

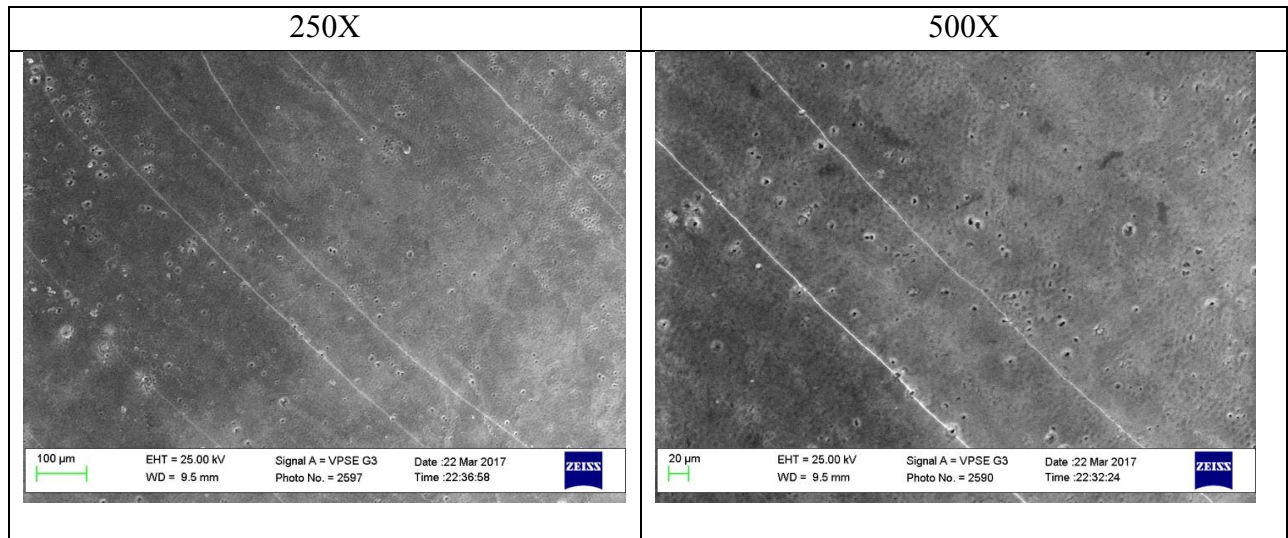
Tooth 10, T1

	250X	500X
Location A	 <p>100 μm EHT = 25.00 kV Signal A = VPSE G3 Date : 8 Mar 2017 WD = 8.0 mm Photo No. = 2431 Time : 3:28:48 ZEISS</p>	 <p>20 μm EHT = 25.00 kV Signal A = VPSE G3 Date : 8 Mar 2017 WD = 8.0 mm Photo No. = 2425 Time : 3:21:29 ZEISS</p>
Location B	 <p>100 μm EHT = 25.00 kV Signal A = VPSE G3 Date : 8 Mar 2017 WD = 8.0 mm Photo No. = 2444 Time : 3:42:28 ZEISS</p>	 <p>20 μm EHT = 25.00 kV Signal A = VPSE G3 Date : 8 Mar 2017 WD = 8.0 mm Photo No. = 2438 Time : 3:35:07 ZEISS</p>
Location C	 <p>100 μm EHT = 25.00 kV Signal A = VPSE G3 Date : 8 Mar 2017 WD = 8.0 mm Photo No. = 2454 Time : 3:52:55 ZEISS</p>	 <p>20 μm EHT = 25.00 kV Signal A = VPSE G3 Date : 8 Mar 2017 WD = 8.0 mm Photo No. = 2447 Time : 3:49:27 ZEISS</p>

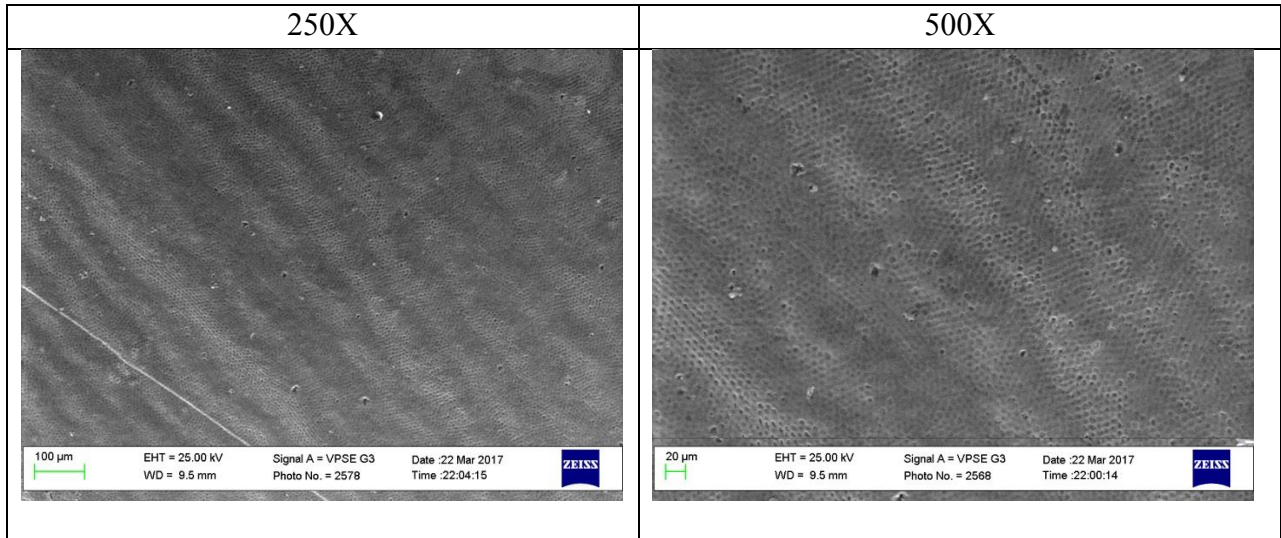
Tooth 10, T2

	250X	500X
Location A	 <p>100 μm EHT = 25.00 kV Signal A = VPSE G3 Date :21 Mar 2017 WD = 8.0 mm Photo No. = 2463 Time :20:58:44 ZEISS</p>	 <p>20 μm EHT = 25.00 kV Signal A = VPSE G3 Date :21 Mar 2017 WD = 8.0 mm Photo No. = 2457 Time :20:51:17 ZEISS</p>
Location B	 <p>100 μm EHT = 25.00 kV Signal A = VPSE G3 Date :21 Mar 2017 WD = 8.0 mm Photo No. = 2474 Time :21:12:28 ZEISS</p>	 <p>30 μm EHT = 25.00 kV Signal A = VPSE G3 Date :21 Mar 2017 WD = 8.0 mm Photo No. = 2469 Time :21:08:43 ZEISS</p>
Location C	 <p>100 μm EHT = 25.00 kV Signal A = VPSE G3 Date :22 Mar 2017 WD = 8.0 mm Photo No. = 2491 Time :3:48:53 ZEISS</p>	 <p>20 μm EHT = 25.00 kV Signal A = VPSE G3 Date :21 Mar 2017 WD = 8.0 mm Photo No. = 2493 Time :21:22:48 ZEISS</p>

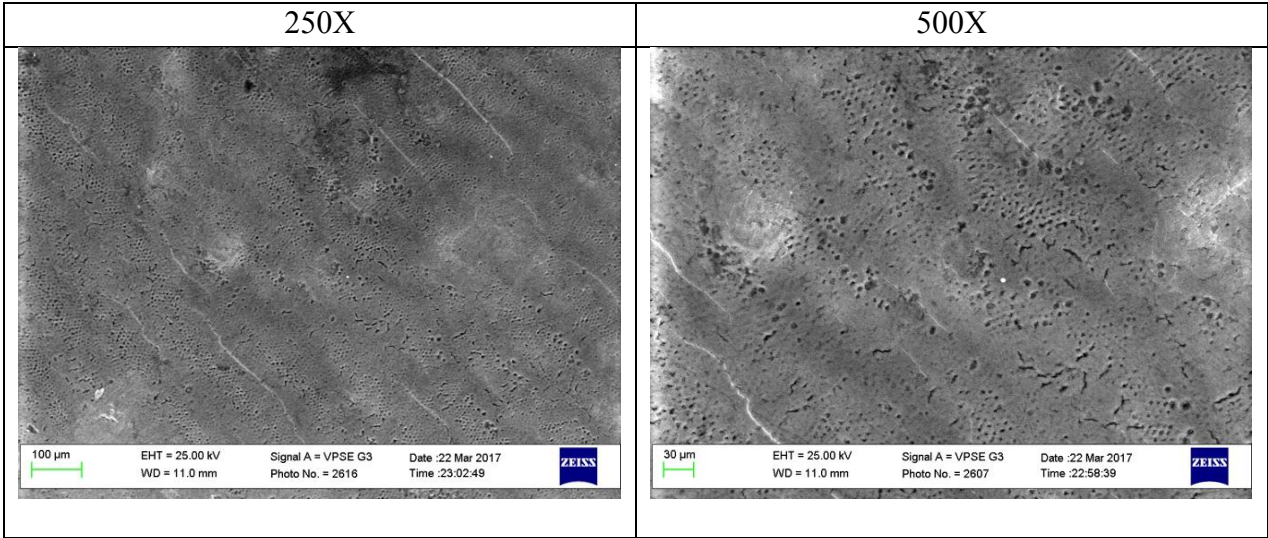
Control A: Sound Enamel



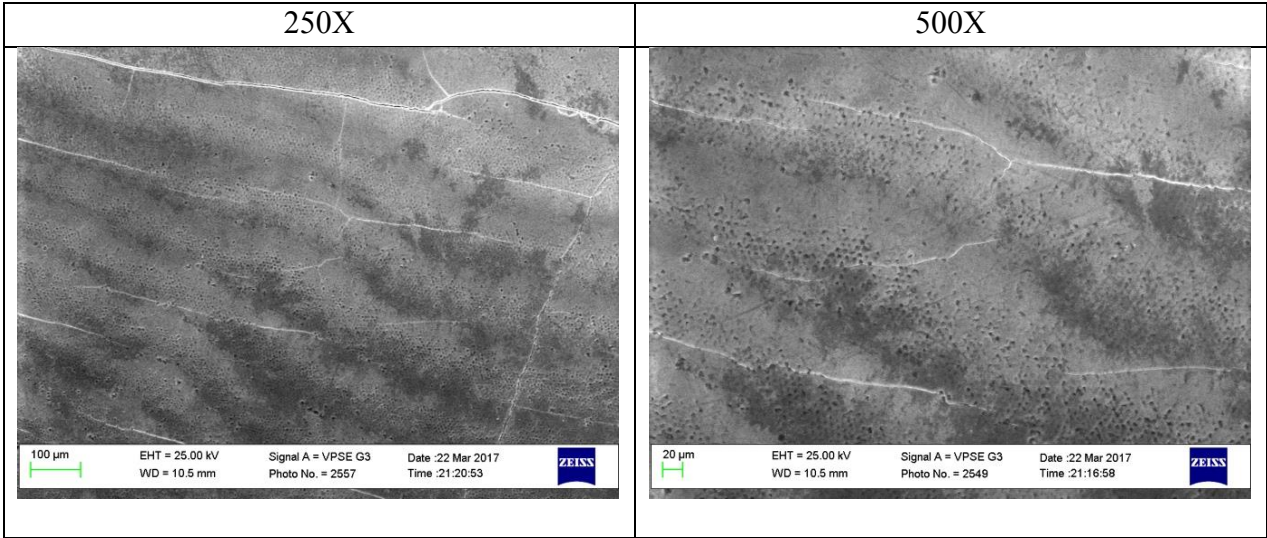
Control B: Sound Enamel



Control C: Demineralized Enamel



Control D: Demineralized Enamel



Vita

Danielle Elizabeth Easterly was born on September 27, 1988 in Fairfax, Virginia. She is currently a citizen of the United States of America. After attending the University of Virginia and receiving a B.A. in Psychology with a minor in Biology in 2010, Dr. Easterly went on to continue her dental education at Virginia Commonwealth University. She earned her Doctorate of Dental Surgery in 2015. She is currently enrolled as a resident in the Virginia Commonwealth University Department of Orthodontics.